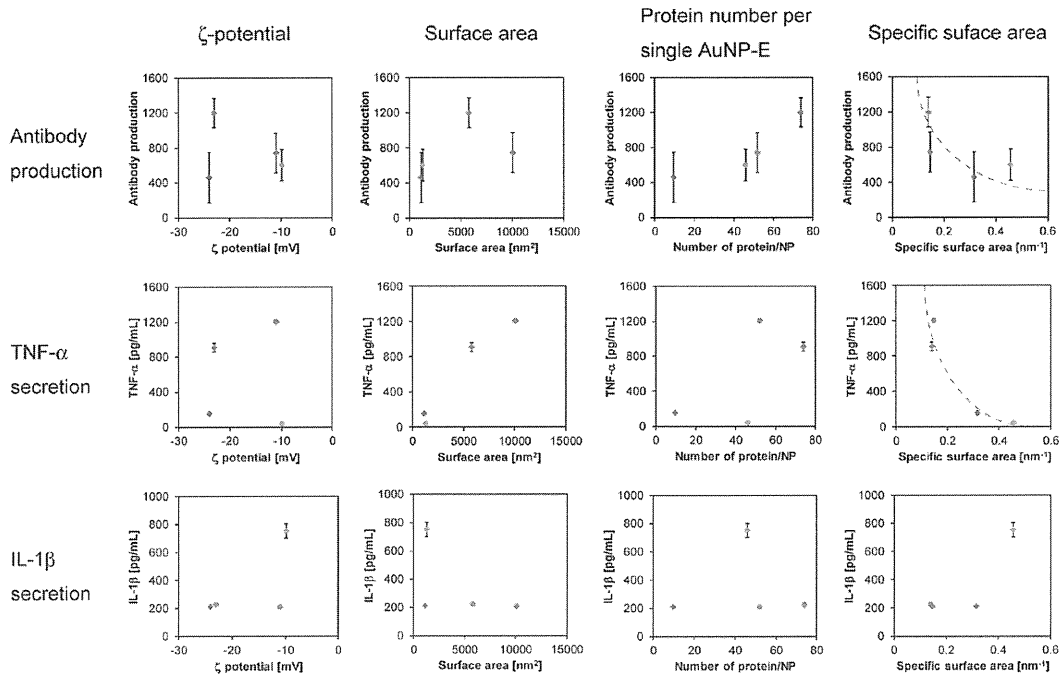

Figure 8. Antibody production or cytokine secretion (TNF-α or IL-1β) *vs* four parameters (ζ-potential, surface area, protein number per single AuNP-E, and specific surface area). Blue, Sphere20-E; red, Sphere40-E; green, Cube-E; orange, Rod-E.

extraction of one specific parameter that dominates immune responses appears difficult. However, we choose four representative parameters for each AuNP-E (surface charge, surface area, protein number per single AuNP-E, and specific surface area, which is the total surface area per single nanoparticle volume (Table S1)) and investigated the correlation between these parameters and antibody production and cytokine secretion (TNF-α or IL-1β) (Figure 8). We note that the specific surface area has an inversely proportional relationship to both antibody production and cytokine secretion. The AuNP-Es with a low specific surface area, such as those with large spherical structures, induced high levels of antibodies and cytokines. In contrast, different effects on antibody and cytokine production were observed for the other parameters. It is known that the size of the spherical nanoparticle presenting the antigen[17] as well as the density of the antigen on the nanoparticle surface[9] is important in producing a strong immune response. On the basis of the above correlations, we propose that specific surface area, which is dependent on both the size and shape of the nanoparticles, is the key factor to simultaneously explain the immune responses observed *in vivo* and *in vitro* in our study. The larger antibody response of Rod-Es compared to that of Sphere20-Es can be explained by the effects of aggregation and their ability to induce high levels of inflammasome-related cytokine secretion. Although the size of nanoparticles has been reported to affect their pharmacokinetics[57−60] and immune responses,[17,22,61] our *in vivo* findings regarding the dependency of immune response on the specific surface area, which is a factor influenced by both size and shape, will be an important factor in the further development of nanoparticle-based vaccines.

CONCLUSIONS

We investigated the effects of shape and size (Sphere40, Sphere20, cube, and rod) of WNVE-coated AuNPs on antibody production in mice. Sphere40 was more effective as a platform than the other shapes (cube and rod) or the smaller sphere (20 nm). For *in vitro* studies using APCs (macrophage and dendritic cells), the rods were most efficiently internalized into these cells and induced the secretion of the inflammasome-related cytokines, IL-1β and IL-18. On the other hand, Sphere40 and cube AuNPs were inefficient for cellular uptake from APCs in comparison to the rods; however, both Sphere40 and cube AuNPs induced the secretion of the pro-inflammatory cytokines, TNF-α, IL-6, IL-12, and GM-CSF, at high levels. We speculated that Sphere40 could efficiently induce antibody production by activating these inflammatory cytokines, whereas rods act *via* inflammasome activation. We note that the specific surface area of AuNPs of various sizes and shapes is a common factor that is correlated to both the secretion of pro-inflammatory cytokines and antibody production. The detailed mechanisms for and generality of the dominant factor underlying the effects of size and shape on immune response, such as aspect ratio, level of protein adsorption, or interaction between nanoparticles and the cell

membrane, should be clarified in a biological environment by further investigation. However, our data for AuNP shape-dependent antibody production and specific cytokine release will contribute to the future design of safe and effective nanoparticle-based vaccines through the activation of the desired immune response.

MATERIALS AND METHODS

Materials. All commercially available reagents were used without further purification. Dulbecco's modified Eagle's medium (DMEM), RPMI-1640, fetal bovine serum (FBS), penicillin, and streptomycin were purchased from GIBCO. The 96-well plates for ELISA were purchased from NUNC (Thermo Fisher Scientific Inc., USA). ECL Western Blotting detection reagents, Precision Plus protein dual color standard, Mini-PROTEAN TGX precast gels, Immun-Blot PVDF membrane and extra thick blot paper were purchased from Bio-Rad Laboratories, Inc. (USA). Mouse anti-WNV envelope IgG and HRP-conjugated anti-mouse IgG were purchased from Abcam plc (UK). IL-1β and TNF-α Quantikine ELISA kits were purchased from R&D Systems, Inc. (USA). IL-18 ELISA kits were purchased from MBL (Japan). Verikine IFN-αELISA kits were purchased from PBL Interferon Source (USA). Other reagents were purchased from Wako Pure Chemical Industries (Japan) and Sigma Aldrich (USA). In all experiments, deionized Millipore water (18 MΩcm^{-1}) was used.

AuNP Synthesis. Gold nanorods (rods) were prepared using a seeding growth method as described previously by Murphy *et al.*[13] Gold nanospheres (20 and 40 nm in a diameter; Sphere20s and Sphere40s, respectively) and nanocubes (cubes) were prepared according to the method reported by Wang *et al.* with modifications,[29] particularly in the case of the nanospheres. Briefly, to a seed solution consisting of $HAuCl_4$ (0.01 M, 250 μL) and CTAB or CTAC (0.1 M, 7.5 mL) was added ice-cold $NaBH_4$ (0.01 M, 600 μL). The resulting seed solution was stirred at room temperature for 2 h. The CTAB-stabilized seeds were used for cube and rod synthesis, and CTAC-stabilized seeds were used for nanosphere synthesis. The growth solution was prepared by the sequential addition of CTAB (0.1 M, 2.9 mL) or CTAB and CTAC (0.1 M, 1.45 mL each), $HAuCl_4$ (0.01 M, 370 μL), and ascorbic acid (0.1 M, 1.8 mL) into water (15 mL). The seed solutions were diluted 10-fold with water. The diluted seed solutions (9.3 μL for Sphere40 and cube, 93 μL for Sphere20) were then added to the growth solution. The resultant solutions were mixed by gentle inversion for 10 s and then left undisturbed overnight at 30 °C.

Scanning transmission electron microscopic (STEM) images were obtained using a STEM HD-2000 system (Hitachi High-Tech Manufacturing & Service Co., Ltd., Japan) with 200 kV accelerating voltage. UV–vis spectra were measured with a UV–vis spectrophotometer (UV-1650PC; Shimadzu Corporation, Japan).

Preparation of West Nile Virus Envelope (WNVE) Protein. Water-soluble His-tagged ectodomain of WNVE protein (NY99 6LP strain) was produced by a persistently expressing 293T cell line. WNVE protein was purified by immobilized metal ion affinity column chromatography with a Ni-NTA column (GE) in accordance with the manufacturer's instructions. The elution fractions were assessed by SDS-PAGE, and those fractions containing WNVE protein were pooled. The purified E protein was then dialyzed overnight at 4 °C against PBS and concentrated using a 30 kDa molecular weight cutoff (MWCO) Amicon-Ultra filter unit (Millipore).

For cell imaging, the WNVE protein was modified with Alexa Fluor 647 carboxylic acid and succinimidyl ester (Life Technologies) by incubation for 1 h at room temperature.

AuNP–Protein Complex (AuNP-E) Preparation. The synthesized AuNP solutions were purified by centrifugation twice using a CF-16RX system (Hitachi-Koki, Ltd., Japan) to remove excess CTAB (2000–4000*g*, 10 min each). According to previous report published by Murphy *et al.*,[30] a poly(4-styrenesulfonic acid-*co*-maleic acid) sodium salt (PSS-MA; 1:1 4-styrenesulfonic acid/maleic acid mole ratio, MW ~ 20 000 g/mol) solution (10 mg/mL, 200 μL) was added to the AuNP solutions (1 mL), and the resultant mixtures were vortexed for 30 s. After adsorption for 1 h, the excess polymer in the supernatant fraction was removed by centrifugation twice (2000–4000*g*, 10 min each) followed by resuspension in water. WNVE protein (10 μg) was added to the polymer-coated AuNP solutions, and the mixtures were incubated at 30 °C for 1 h. After adsorption, the excess protein in the supernatant fraction was removed by centrifugation twice (2000–4000*g*, 10 min each) followed by resuspension in PBS.

Quantification of WNVE Protein on AuNPs. The AuNP-E solutions were concentrated by centrifugation and then added to SDS-PAGE sample buffer to peel off proteins from the surface of the AuNPs. After heating at 95 °C for 5 min for denaturation of the proteins, the solutions were centrifuged (6000*g*, 5 min) to completely precipitate the AuNPs. The supernatants were applied to SDS-PAGE with WNVE protein of known concentrations and then transferred to a PVDF membrane using a semidry method. The transferred membrane was analyzed by Western blotting with mouse anti-WNV envelope IgG and HRP-conjugated anti-mouse IgG. Immunoreactive proteins were detected with ECL detection reagent and quantified by densitometry using a LAS-3000 imaging system (FUJIFILM, Japan).

Absorbance and Dynamic Light Scattering (DLS) Measurement in Biological Medium. The AuNP-E solutions were added to DMEM supplemented with 10% fetal bovine serum (FBS) and incubated for 24 h. At 0, 6, and 24 h, absorbance spectra and hydrodynamic diameters were measured using a UV–vis spectrophotometer and Delsa Nano HC (Beckman Coulter, USA).

Immunization and Analysis of Antibody Responses. Groups of ten 4-week-old female C3H/HeNJc1 mice (CLEA Japan, Inc., Japan) were intraperitoneally immunized twice at 3 week intervals with 100 ng protein/animal of AuNP-Es, PBS, or WNVE protein solution. Sera were collected at 1 week after the second immunization. The anti-WNVE immunoglobulin G (IgG) titers of the individual mouse sera were determined using ELISA plates coated with WNVE protein and HRP-conjugated antimouse IgG. Immunoreactive proteins were detected with SIGMAFAST OPD. After reaction, the absorbance at 450 nm was measured. Absorbance cutoff values were calculated as the mean absorbance of sera from PBS-immunized mice. Antibody production was expressed as the reciprocal of the maximum dilution giving an absorbance greater than the cutoff value.

Generation of BMDCs. Bone-marrow-derived dendritic cells (BMDCs) were generated from mouse BM as previously described.[62,63] In brief, BM cells of 6-week-old male C3H/HeNJc1 mice were depleted of T cells, B cells, macrophages, and granulocytes by killing with lineage-specific antibodies and complement. Subsequently, the cells were cultured in RPMI-1640 supplemented with 10% FBS, 10 ng/mL recombinant mouse granulocyte/macrophage colony-stimulating factor (rmGM-CSF; R&D Systems), and 50 μM β-mercaptoethanol for 6 days in 24-well culture plates. The culture medium was changed for fresh medium every 2 days. We usually acquired 4×10^6 immature DCs from each mouse.

Cell Culture and Treatment with AuNP-Es. RAW264.7 cells were maintained in DMEM supplemented with 10% FBS, 500 units/mL penicillin, and 500 μg/mL streptomycin. Cells were seeded at 10^5 cells/well in 6-well cell culture plate or 35 mm glass-bottomed dishes (Asahi Glass Co. Ltd., Japan) and treated 24 h later. In the case of BMDCs, cells were seeded at 10^5 cells/well in triple-well glass-based dishes. The cultures were kept at 37 °C in a humidified incubator under a 5% CO_2 atmosphere.

In cell imaging experiments, AuNP-Es conjugated with Alexa Fluor 647 were added to the cell dishes at a final concentration at 5×10^{10} NPs/mL. After incubation in an incubator for 1.5 h, the cells were washed with PBS three times to remove AuNP-Es that did not enter the cells and then added to fresh culture medium. For colocalization observation of AuNP-Es and lysosomes, 50 nM Lysotracker Blue DND-22 in cell culture medium

was added. After incubation for 30 min, cells were washed with PBS three times and added to fresh medium. These cell samples were then ready for imaging measurements. Fluorescence and differential interference contrast (DIC) images were obtained using a confocal laser scanning microscope (CLMS; Olympus FV-300). The cell imaging experiments were done under same conditions, including laser power and photomultiplier gain, on the same day. In BMDC imaging experiments, BMDCs were treated with 10 μg/mL AuNP-Es for 24 h. After exposure to AuNP-Es, cell culture supernatants were removed and 0.2 μg/mL Hoechst in cell culture medium was added. After incubation for 20 min, cells were washed with PBS three times and added to fresh culture medium.

In cellular uptake and removal experiments, AuNP-Es were added to the cell dishes under the same conditions as in the cell imaging experiments, and washing was performed in the same manner. For the removal experiment, the cells were cultured for a further 48 h and washed three times. The cells were treated with aqua regia, and the cell dispersion was further sonicated for 1 min to completely disrupt the cell membranes and dissolve AuNPs to gold ions. The resultant solutions were diluted with water (6 mL). The concentrations of gold ions in the cells were determined by ICP-AES (ICPE-9000, Shimadzu) after obtaining a calibration curve for the gold ions at various concentrations using commercial standards. The concentrations of gold ions contained in the cells were then converted to the number of gold nanoparticles taken up per cell by consideration of the size of the nanoparticles obtained from the STEM imaging and the total number of cells involved.

TEM Observation. RAW264.7 cells were incubated with the AuNP-Es (final concentration: 2 μg/mL) for 3 h in DMEM on BioCoat poly-D-lysine 8-well CultureSlides (BD). After washing with PBS buffer, the cells were fixed in 2.5% glutaraldehyde/0.1 M phosphate buffer (pH 7.4) overnight at 4 °C, postfixed in a mixed aqueous solution of 1% osmium tetroxide and 1.5% potassium ferrocyanide for 2 h at room temperature, dehydrated in a graded ethanol series, and embedded in Epon 812 (TAAB). Ultrathin sections were then cut on a RMC Ultramicrotome MTX. The sections were stained with uranyl acetate followed by lead citrate and examined at 80 kV with a JEM-1400 transmission electron microscope (JEOL, Japan).

Cytokine Production Measurement. BMDCs were first primed with 50 ng/mL LPS for 3 h. After priming, the cells were seeded at 10^5 cells/well in 96-well cell culture plate. The cells were then treated with 50 ng/mL LPS and AuNP-Es at various concentrations for 24 h. The level of IL-1β and IL-18 was measured by ELISA following the manufacturer's protocols. For several cytokine and chemokine measurements, BMDCs were not primed with LPS. Culture supernatants were collected and tested for cytokine levels by LUMINEX (IL-6, IL-12, and GM-CSF) using the mouse cytokine Ten-Plex antibody bead kit (Invitrogen) or ELISA (TNF-α and INF-α) following the manufacturer's protocols.

Cytotoxity Assay. Cells were seeded at 10^4 cells/well (RAW264.7 cell) or 10^5 cells/well (BMDC) in 96-well cell culture plates. Cell viability was tested using a cell-counting kit 8 (CCK-8, Dojindo, Japan). After incubation for 24 h with AuNPs, the medium was removed, and fresh medium (100 μL) containing 10% CCK-8 reagent was added to each well. The culture plates were incubated at 37 °C and 5% CO_2 for 3 h. After incubation, the absorbance at 450 nm was measured using a microplate reader (Infinite 200 PRO, Tecan).

Statistical Analysis. Statistical analysis was carried out using Student's independent *t* test. A value of $p < 0.05$ was considered to be significant.

Conflict of Interest: The authors declare no competing financial interest.

Acknowledgment. We gratefully acknowledge the Cabinet Office, Government of Japan and the Japan Society for the Promotion of Science (JSPS) for financial support through the FIRST Program, grants from the Ministry of Education, Culture, Sports, Science, and Technology (MEXT) and the Ministry of Health, Labor and Welfare, Japan. A part of this work was conducted at Hokkaido Innovation through Nanotechnology Support (HINTS), supported by "Nanotechnology Network JAPAN" Program and the Japan Initiative for Global Research Network on Infectious Diseases (J-GRID), MEXT Japan.

Supporting Information Available: Figure S1–S7 and Table S1 as described in the text. This material is available free of charge *via* the Internet at http://pubs.acs.org.

REFERENCES AND NOTES

1. Harris, J. R.; Markl, J. Keyhole Limpet Hemocyanin (KLH): A Biomedical Review. *Micron* **1999**, *30*, 597–623.
2. Ragupathi, G.; Meyers, M.; Adluri, S.; Howard, L.; Musselli, C.; Livingston, P. O. Induction of Antibodies against GD3 Ganglioside in Melanoma Patients by Vaccination with GD3-Lactone-KLH Conjugate Plus Immunological Adjuvant QS-21. *Int. J. Cancer* **2000**, *85*, 659–666.
3. Hou, Y.; Gu, X. X. Development of Peptide Mimotopes of Lipooligosaccharide from Nontypeable *Haemophilus influenza* as Vaccine Candidates. *J. Immunol.* **2003**, *170*, 4373–4379.
4. May, R. J.; Beenhouwer, D. O.; Scharff, M. D. Antibodies to Keyhole Limpet Homecyanin Cross-React with an Epitope on the Polysaccharide Capsule of *Cryptococcus neoformans* and Other Carbohydrates: Implications for Vaccine Development. *J. Immunol.* **2003**, *171*, 4905–4912.
5. Gharavi, A. E.; Pierangeli, S. S.; Stanfield, M. C.; Liu, X. W.; Espinola, R. G.; Harris, E. N. GDKV-Induced Antiphospholipid Antibodies Enhance Thrombosis and Activate Endothelial Cells *in Vivo* and *in Vitro*. *J. Immunol.* **1999**, *163*, 2922–2927.
6. Chen, Y. S.; Hung, Y. C.; Lin, W. H.; Huang, G. S. Assessment of Gold Nanoparticles as a Size-Dependent Vaccine Carrier for Enhancing the Antibody Response against Synthetic Foot-and-Mouth Disease Virus Peptide. *Nanotechnology* **2010**, *21*, 195101–1951018.
7. Rana, S.; Bajaj, A.; Mout, R.; Rotello, V. M. Monolayer Coated Gold Nanoparticles for Delivery Applications. *Adv. Drug Delivery Rev.* **2012**, *64*, 200–216.
8. De, M.; Ghosh, P. S.; Rotello, V. M. Applications of Nanoparticles in Biology. *Adv. Mater.* **2008**, *20*, 4225–4241.
9. Bastús, N. G.; Sánchez-Tilló, E.; Pujals, S.; Farrera, C.; López, C.; Giralt, E.; Celada, A.; Lloberas, J.; Puntes, V. Homogeneous Conjugation of Peptides onto Gold Nanoparticles Enhances Macrophage Response. *ACS Nano* **2009**, *3*, 1335–1344.
10. Shukla, R.; Bansal, V.; Chaudhary, M.; Basu, A.; Bhonde, R. R.; Sastry, M. Biocompatibility of Gold Nanoparticles and Their Endocytotic Fate Inside the Cellular Compartment: A Microscopic Overview. *Langmuir* **2005**, *21*, 10644–10654.
11. Dykman, L.; Khlebtsov, N. Gold Nanoparticles in Biomedical Applications: Recent Advances and Perspectives. *Chem. Soc. Rev.* **2013**, *41*, 2256–2282.
12. Perrault, S. D.; Chan, W. C. W. Synthesis and Surface Modification of Highly Monodispersed, Spherical Gold Nanoparticles of 50–200 nm. *J. Am. Chem. Soc.* **2009**, *131*, 17042–17043.
13. Sau, T. K.; Murphy, C. J. Room Temperature, High-Yield Synthesis of Multiple Shapes of Gold Nanoparticles in Aqueous Solution. *J. Am. Chem. Soc.* **2004**, *126*, 8648–8649.
14. Shiosaka, S.; Kiyami, H.; Wanaka, A.; Tohyama, M. A New Method for Producing a Specific and High Titre Antibody against Glutamate Using Colloidal Gold as a Carrier. *Brain Res.* **1986**, *382*, 399–403.
15. Chen, Y. S.; Hung, Y. C.; Liau, I.; Huang, G. S. Assessment of the *In Vivo* Toxicity of Gold Nanoparticles. *Nanoscale Res. Lett.* **2009**, *4*, 858–864.
16. Jiang, W.; Kim, B. Y. S.; Rutka, J. T.; Chan, W. C. W. Nanoparticle-Mediated Cellular Response Is Size-Dependent. *Nat. Nanotechnol.* **2008**, *3*, 145–150.
17. Mottram, P. L.; Leong, D.; Irwin, B. C.; Gloster, S.; Xiang, S. D.; Meanger, J.; Ghildyal, R.; Vardaxis, N.; Plebanski, M. Type 1 and 2 Immunity Following Vaccination Is Influenced by Nanoparticle Size: Formulation of a Model Vaccine for

Respiratory Syncytial Virus. *Mol. Pharmaceutics* **2007**, *4*, 73–84.
18. Wang, Y. T.; Lu, X. M.; Zhu, F.; Huang, P.; Yu, Y.; Zeng, L.; Long, Z. Y.; Wu, Y. M. The Use of a Gold Nanoparticle-Based Adjuvant To Improve the Therapeutic Efficacy of hNgR-Fc Protein Immunization in Spinal Cord-Injured Rats. *Biomaterials* **2011**, *32*, 7988–7998.
19. Banchereau, J.; Briere, F.; Caux, C.; Davoust, J.; Lebecque, S.; Liu, Y. J.; Pulendran, B.; Palucka, K. Immunobiology of Dendritic Cells. *Annu. Rev. Immunol.* **2000**, *18*, 767–811.
20. Janeway, C. A., Jr.; Medzhitov, R. Innate Immune Recognition. *Annu. Rev. Immunol.* **2002**, *20*, 197–216.
21. Hubbell, J. A.; Thomas, S. N.; Swartz, M. A. Materials Engineering for Immunomodulation. *Nature* **2009**, *462*, 449–460.
22. Yen, H. J.; Hsu, S. H.; Tsai, C. L. Cytotoxicity and Immunological Response of Gold and Silver Nanoparticles of Different Sizes. *Small* **2009**, *5*, 1553–1561.
23. Hutter, E.; Boridy, S.; Labrecque, S.; Hebert, M. L.; Kriz, J.; Winnik, F. M.; Maysinger, D. Microglial Response to Gold Nanoparticles. *ACS Nano* **2010**, *4*, 2595–2606.
24. Dauphin, G.; Zientara, S. West Nile Virus: Recent Trends in Diagnosis and Vaccine Development. *Vaccine* **2007**, *25*, 5563–5576.
25. Chithrani, B. D.; Chan, W. C. W. Elucidating the Mechanism of Cellular Uptake and Removal of Protein-Coated Gold Nanoparticles of Different Sizes and Shapes. *Nano Lett.* **2007**, *7*, 1542–1550.
26. Fifis, T.; Gamvrellis, A.; Irwin, B. C.; Pietersz, G. A.; Li, J.; Mottram, P. L.; Mckenzie, I. F. C.; Plebanski, M. Size-Dependent Immunogenicity: Therapeutic and Protective Properties of Nano-Vaccines against Tumors. *J. Immunol.* **2004**, *173*, 3148–3154.
27. Chithrani, B. D.; Ghazani, A. A.; Chan, W. C. W. Determining the Size and Shape Dependence of Gold Nanoparticle Uptake into Mammalian Cells. *Nano Lett.* **2006**, *6*, 662–668.
28. Mukhopadhyay, S.; Kim, B. S.; Chipman, P. R.; Rossmann, M. G.; Kuhn, R. J. Structure of West Nile Virus. *Science* **2003**, *302*, 248.
29. Chen, H.; Kou, X.; Yang, Z.; Ni, W.; Wang, J. Shape- and Size-Dependent Refractive Index Sensitivity of Gold Nanoparticles. *Langmuir* **2008**, *24*, 5233–5237.
30. Gole, A.; Murphy, C. J. Azide-Derivatized Gold Nanorods: Functional Materials for "Click" Chemistry. *Langmuir* **2008**, *24*, 266–272.
31. Kanai, R.; Kar, K.; Anthony, K.; Gould, L. H.; Ledizet, M.; Fikrig, E.; Marasco, W. A.; Koski, R. A.; Modis, Y. Crystal Structure of West Nile Virus Envelope Glycoprotein Reveals Viral Surface Epitopes. *J. Virol.* **2006**, *80*, 11000–11008.
32. Walkey, C. D.; Chan, W. C. W. Understanding and Controlling the Interaction of Nanomaterials with Proteins in a Physiological Environment. *Chem. Soc. Rev.* **2012**, *41*, 2780–2799.
33. Casal, E.; Pfaller, T.; Duschl, A.; Oostingh, G. J.; Puntes, V. Time Evolution of the Nanoparticle Protein Corona. *ACS Nano* **2010**, *4*, 3623–3632.
34. Monopoli, M.; Åberg, C.; Salvati, A.; Dawson, K. A. Biomolecular Coronas Provide the Biological Identity of Nanosized Materials. *Nat. Nanotechnol.* **2012**, *7*, 779–786.
35. Maiorano, G.; Sabella, S.; Sorce, B.; Brunetti, V.; Malvindi, M. A.; Cingolani, R.; Pompa, P. P. Effects of Cell Culture Media on the Dynamic Formation of Protein–Nanoparticle Complexes and Influence on the Cellular Response. *ACS Nano* **2010**, *4*, 7481–7491.
36. Gil, P. R.; Oberdörster, G.; Elder, A.; Puntes, V.; Parak, W. J. Correlating Physico-Chemical with Toxicological Properties of Nanoparticles: The Present and the Future. *ACS Nano* **2010**, *4*, 5527–5531.
37. Ohatki, N.; Takahashi, H.; Kaneko, K.; Gomi, Y.; Ishikawa, T.; Higashi, Y.; Kurata, T.; Sata, T.; Kojima, A. Immunogenicity and Efficacy of Two Types of West Nile Virus-like Particles Different in Size and Maturation as a Second-Generation Vaccine Candidate. *Vaccine* **2010**, *28*, 6588–6596.
38. Raschke, W. C.; Baird, S.; Ralph, P.; Nakoinz, I. Functional Macrophage Cell Lines Transformed by Abelson Leukemia Virus. *Cell* **1978**, *15*, 261–267.
39. Hauck, T. S.; Ghazani, A. A.; Chan, W. C. W. Assessing the Effect of Surface Chemistry on Gold Nanorod Uptake, Toxicity, and Gene Expression in Mammalian Cells. *Small* **2008**, *4*, 153–159.
40. Walkey, C. D.; Olsen, J. B.; Guo, H.; Emili, A.; Chan, W. C. W. Nanoparticle Size and Surface Chemistry Determine Serum Protein Adsorption and Macrophage Uptake. *J. Am. Chem. Soc.* **2012**, *134*, 2139–2147.
41. Arnida; Janát-Amsbury, M. M.; Ray, A.; Peterson, C. M.; Ghandehari, H. Geometry and Surface Characteristics of Gold Nanoparticles Influence Their Biodistribution and Uptake by Macrophages. *Eur. J. Pharm. Biopharm.* **2011**, *77*, 417–423.
42. Vácha, R.; Martinez-Veracoechaea, F. J.; Frenkel, D. Receptor-Mediated Endocytosis of Nanoparticles of Various Shapes. *Nano Lett.* **2011**, *11*, 5391–5395.
43. Ghiringhelli, F.; Apetoh, L.; Tesniere, A.; Aymeric, L.; Ma, Y.; Ortiz, C.; Vermaelen, K.; Panaretakis, T.; Mignot, G.; Ullrich, E.; *et al.* Activation of the NLRP3 Inflammasome in Dendritic Cells Induces IL-1β-Dependent Adaptive Immunity against Tumors. *Nat. Med.* **2009**, *15*, 1170–1178.
44. Martinon, F.; Mayor, A.; Tschopp, J. The Inflammasomes: Guardians of the Body. *Annu. Rev. Immunol.* **2009**, *27*, 229–265.
45. Lunov, O.; Syrovets, T.; Loos, C.; Nienhaus, G. U.; Mailänder, V.; Landfester, K.; Rouis, M.; Simmet, T. Amino-Functionalized Polystyrene Nanoparticles Activate the NLRP3 Inflammasome in Human Macrophages. *ACS Nano* **2011**, *5*, 9648–9657.
46. Yang, E. J.; Kim, S.; Kim, J. S.; Choi, I. H. Inflammasome Formation and IL-1β Release by Human Blood Monocytes in Response to Silver Nanoparticles. *Biomaterials* **2012**, *33*, 6858–6867.
47. Hornung, V.; Bauernfeind, F.; Halle, A.; Samstad, E. O.; Kono, H.; Rock, K. L.; Fitzgerald, K. A.; Latz, E. Silica Crystals and Aluminum Salts Activate the NALP3 Inflammasome through Phagosomal Destabilization. *Nat. Immunol.* **2008**, *9*, 847–856.
48. Vácha, R.; Martinez-Veracoechaea, F. J.; Frenkel, D. Intracellular Release of Endocytosed Nanoparticles upon a Change of Ligand–Receptor Interaction. *ACS Nano* **2012**, *6*, 10598–10605.
49. Dinarello, C. A. Biologic Basis for Interleukin-1 in Disease. *Blood* **1996**, *87*, 2095–2147.
50. Zhou, R.; Yazdi, A. S.; Menu, P.; Tschopp, J. A Role for Mitochondria in NLRP3 Inflammasome Activation. *Nat. Immunol.* **2011**, *12*, 199–200.
51. Eisenbarth, S. C.; Colegio, O. R.; O'Connor, W., Jr.; Sutterwala, F. S.; Flavell, R. A. Crucial Role for the Nalp3 Inflammasome in the Immunostimulatory Properties of Aluminium Adjuvants. *Nature* **2008**, *453*, 1122–1126.
52. Li, H.; Willingham, S. B.; Ting, J. P. Y.; Re, F. Cutting Edge: Inflammasome Activation by Alum and Alum's Adjuvant Effect are Mediated by NLRP3. *J. Immunol.* **2008**, *181*, 17–21.
53. Wickliffe, K. E.; Leppla, S. H.; Moayeri, M. Anthrax Lethal Toxin-Induced Inflammasome Formation and Caspase-1 Activation Are Late Events Dependent on Ion Fluxes and the Proteasome. *Cell. Microbiol.* **2008**, *10*, 332–343.
54. Wajant, H.; Pfizenmaier, K.; Scheurich, P. Tumor Necrosis Factor Signaling. *Cell Death Differ.* **2003**, *10*, 45–65.
55. Franchi, L.; Núñez, G. The Nlrp3 Inflammasome Is Critical for Aluminiumhydroxide-Mediated IL-1β Secretion but Dispensable for Adjuvant Activity. *Eur. J. Immunol.* **2008**, *38*, 2085–2089.
56. Bon, A. L.; Schiavoni, G.; D'Agostin, G.; Gresser, I.; Belardelli, F.; Tough, D. F. Type I Interferons Potently Enhance Humoral Immunity and Can Promote Isotype Switching by Stimulating Dendritic Cells *in Vivo*. *Immunity* **2001**, *14*, 461–470.
57. Thakor, A. S.; Jokerst, J.; Zavaleta, C.; Massoud, T. F.; Gambhir, S. S. Gold Nanoparticles: A Revival in Precious Metal Administration to Patients. *Nano Lett.* **2011**, *11*, 4029–4036.
58. Alkilany, A. M.; Lohse, S. E.; Murphy, C. J. The Gold Standard: Gold Nanoparticle Libraries To Understand the Nano–Bio Interface. *Acc. Chem. Res.* **2013**, *46*, 650–661.

59. Alkilany, A. M.; Murphy, C. J. Toxicity and Cellular Uptake of Gold Nanoparticles: What We Have Learned So Far? *J. Nanopart. Res.* **2010**, *12*, 2313–2333.
60. Zhou, C.; Long, M.; Qin, Y.; Sun, X.; Zheng, J. Luminescent Gold Nanoparticles with Efficient Renal Clearance. *Angew. Chem., Int. Ed.* **2011**, *50*, 3168–3172.
61. Sharp, F. A.; Ruane, D.; Claass, B.; Creagh, E.; Harris, J.; Malyala, P.; Singh, M.; O'Hagan, D. T.; Pétrilli, V.; Tschopp, J.; *et al.* Uptake of Particulate Vaccine Adjuvants by Dendritic Cells Activates the NALP3 Inflammasome. *Proc. Natl. Acad. Sci. U.S.A.* **2009**, *106*, 870–875.
62. Inaba, K.; Inaba, M.; Romani, N.; Aya, H.; Deguchi, M.; Ikehara, S.; Muramatsu, S.; Steinman, R. M. Generation of Large Numbers of Dendritic Cells from Mouse Bone Marrow Cultures Supplemented with Granulocyte/Macrophage Colony-Stimulating Factor. *J. Exp. Med.* **1992**, *176*, 1693–1702.
63. Kajino, K.; Nakamura, I.; Bamba, H.; Sawai, T.; Ogasawara, K. Involvement of IL-10 in Exhaustion of Myeloid Dendritic Cells and Rescue by CD40 Stimulation. *Immunology* **2007**, *120*, 28–37.

「病理と臨床」31巻2号146-150　2013年

感染症と癌、病理からのメッセージ

7．HTLV-1と白血病・リンパ腫

鈴木　忠樹、長谷川　秀樹（国立感染症研究所　感染病理部）

はじめに

ヒトT細胞白血病ウイルスI型（Human T-cell leukemia virus type I; HTLV-1）は1980年に初めてのヒトの白血病ウイルスとして発見されたレトロウイルスである[1]。一方、成人T細胞白血病・リンパ腫（Adult T-cell leukemia; ATL）は、ウイルスの発見に先立ち1977年に高月らによって報告された疾患概念であり[2]、ウイルスの発見後、HTLV-1はATLの原因ウイルスであることが実験的に証明され、現在ではATLは「HTLV-1感染細胞が腫瘍性増殖を示したもの」と定義されている[3]。HTLV-1は、日本、アフリカ、カリブ海地域、南米を中心として全世界に数千万のウイルスキャリアが存在する。2007年に厚生労働省の研究班が行った全国調査によると日本には約108万人のキャリアが存在している[3]。HTLV-1の主な感染経路は母乳による垂直感染と性交渉もしくは輸血による水平感染である。垂直感染によるキャリアの数%が約60年の長期の潜伏期の後にATLを発症し、日本では毎年1000人以上がATLと診断されている。HTLV-1はATLの他、HTLV-1関連脊髄症（HTLV-1 associated myelopathy / tropical spastic paraparesis; HAM/TSP)、HTLV-1ぶどう膜炎（HTLV-1 uveitis / HTLV-1 associated uveitis; HU/HAU)の原因ウイルスとして知られているが、キャリアからの発症率はATLが最も高い。我が国の基礎および臨床研究者は、ATLの発見、ウイルスの同定、ウイルス遺伝子の構造解明などウイルス学、分子生物学、免疫学、疫学など多方面からの研究に多大な貢献をしてきた。その結果、疫学的研究やHTLV-1の分子生物学的解析、ATLの病態解析は長足の進歩をみせたが、発癌機構には未だに多くの謎が残されており、治療法の確立も途上である。本稿では、HTLV-1による感染細胞の腫瘍化機構を概説し、病理学研究の立場から動物モデルを用いた生体内におけるATL発癌機構研究の最近の伸展について述べる。なお、ATLの病理臨床に関しては詳細な和文総説[4]があるので、そちらを参照されたい。

HTLV-1による感染細胞の腫瘍化

HTLV-1のコードする遺伝子には、レトロウイルスに共通のGag、Pol、Envの構造タンパク質に加えて、TaxおよびRexという調節タンパク質、およびp12[I]、p13[II]、p30[II]のアクセサリータンパク質、およびアンチセンスから転写されるHBZが存在する。HTLV-1感染の特徴は自らのコピー数を増やすために感染細胞内に大量にウイルス粒子を産生するのではなく、宿主細胞の増殖や生存を促すことにより、感染細胞ごとコピー数を増やそうとするところにある。そのためウイルスのコードするタンパク質はウイルスを構成する因子となるだけでなく宿主細胞に対し

て様々な作用を及ぼすことになる。これらのタンパク質の中で感染細胞の不死化と形質転換に最も重要と考えられているのがTaxである。

Taxは分子量40kDaのリン酸化タンパク質であり、主に核内に局在する。ウイルス複製の観点から見ると、Taxはウイルス遺伝子の強力な転写活性化因子である。一方、宿主細胞に対するTaxの作用は、宿主細胞遺伝子発現の脱制御とシグナル伝達系の活性化を通じた細胞増殖とアポトーシス抑制、DNA修復機構の抑制と染色体異常の誘発によるゲノム不安定性の誘導という腫瘍化過程として一般的に知られているものであり、腫瘍化のイニシエーションに関わると考えらえられている。最近、Taxに加えてHBZがHTLV-1による発癌機序の一翼を担うことが明らかにされたが、依然、主要な発癌のプレーヤーはTaxであると考えられている。

これまでの分子生物学的解析により感染細胞内でのTaxの振る舞いは明らかになってきたが、ATLの発症には長い潜伏期間を要し、感染者の大多数が終生無症候性キャリアであること、さらには多くのATL患者の白血病細胞ではTaxの発現が抑制されており、上述のような*In vitro*の実験で明らかにされたTaxの機能のみでHTLV-1による発癌機構を説明することは困難である。ATL患者の統計学的解析からは、ATL発症は少なくとも５つの遺伝子学的変化の蓄積する多段階発癌モデルに合致することが知られているが、発癌に至るまでに蓄積される遺伝子学的変化とTaxの機能との関係性などについてはいまなお不明である。また、同種造血幹細胞移植を行ったATL患者においては、移植後の寛解維持とTax特異的CTL活性の亢進との関連性を指摘する報告もあり、HTLV-1感染細胞に対する免疫監視機構がATLの発症と極めて密接な関係があると考えられている。このように多段階発癌や宿主免疫との相互作用など長い潜伏期間の間に生体内で起こっていることを明らかにし、真に有効な治療法を確立するためには適切な動物モデルが必要不可欠となる。

HTLV-1感染動物モデル

感染症の動物モデルとは、対象病原体に感受性のある動物を用いてヒトの疾患と類似の病態を再現させるものである。ひとたび動物モデルが構築されると、病態や発症機構の詳細な解析ができるだけでなく予防法や治療法の確立も可能となる。しかしながら、どのような動物モデルでもヒトと異なる生物を用いている以上、完全にヒトで起こっていることを再現することは不可能であり、そのモデルで再現される事象と実際の病態とは異なる事象をよく理解した上で研究に用いることが重要である。

HTLV-1は、マウスを除くほとんどの動物に感染することができ、サル、ウサギ、ラット、ハムスター、ネコなどの動物で感染モデルが作られてきた。サルとウサギを用いた感染モデルは、経口感染や性行為や輸血による感染といずれの系においても感染が成立し、HTLV-1感染様式の証明に有用であった。また、遺伝学的に確立された多数の近交系が存在するラットは有用なHTLV-1感染モデルとして用いられており、WKAという系統のラットはヒトのHAM / TSPに類似した疾患を発症することが知られている。しかしながら、いずれの動物においてもATL様の疾患は再現されていない[5]。

ATL マウスモデルの構築

上述のような HTLV-1 感染動物モデルは、HTLV-1 感染症を理解するためには必要不可欠であるが、HTLV-1 による発癌を再現できない。そこで、発癌機構にのみに着目したウイルス遺伝子トランスジェニック動物による病態モデルを用いた研究が行われている。前述の様に HTLV-1 による発癌機構には Tax が重要な働きをしていることが明らかになっていることから、我々は、T 細胞性白血病・リンパ腫のモデルを作製する目的で HTLV-1 の tax 遺伝子を lck 近位プロモーター下に発現させる HTLV-1 Tax トランスジェニックマウス(Tax tg マウス)を作製した[6]。得られた Tax Tg マウスは生後 10〜23 ヶ月経過した後に肝脾腫、リンパ節腫脹、腸間膜腫瘍を発症し、さらには白血病を発症した。組織学的には、盛んな分裂像を伴うびまん性大細胞性リンパ腫の像を呈し腫瘍細胞は肝臓、脾臓、肺、腎臓、皮膚への浸潤がみられた。白血化した個体の末梢血中に見られる白血病細胞は過分葉してクロマチンの濃縮した核を持つ ATL に特徴的な「花弁細胞 (flower cell)」様であった (図)。この白血病細胞の表面抗原は細胞質内 CD3(+)、CD4(-)、CD8(-)の pre-T 細胞由来の腫瘍であったが、ATL で強発現している CD25、CD69 も陽性であり、さらに、この細胞においては HTLV-1 による形質転換に重要な働きをしている NF-κB が活性化しているなどヒトで起こる ATL と非常に良く似た病態を呈し、ATL の良い病態モデルになると考えられている。我々はこの ATL マウスモデルを用いて *In vivo* で効果的な ATL の新たな治療標的の探索をしている。

ATL マウスモデルを用いた新規治療標的の探索

進行した ATL では皮膚、骨髄、脾臓、肝臓、肺および脳等の多臓器へ白血病細胞が浸潤することが知られている。しかし、ATL 細胞の浸潤メカニズムはこれまでほとんど分かっていなかった。白血病を発症した Tax Tg マウスではヒト ATL と同様、血管周囲性に著明な白血病細胞の浸潤を認めたことから、Tax により誘導された白血病細胞に固有の腫瘍細胞浸潤のメカニズムが存在する可能性が考えられた。そこで、mATL 細胞を用いて腫瘍細胞の走化性機構の解明を試みた。その結果、mATL 細胞の走化性には SDF-1α/CXCR4 経路の関与が示唆された[7]。さらに、この経路はヒト ATL 症例由来の白血病細胞の走化性にも関わっていることが明らかとなった。そこで mATL 細胞を免疫不全マウスに移植し、CXCR4 拮抗薬である AMD3100 を投与したところ、肺、および肝臓への白血病細胞浸潤が抑制された。以上のことから SDF-1α/CXCR4 経路を阻害する AMD3100 は、ATL 細胞浸潤を抑制する新しい治療薬の候補となると考えられた。

ATL マウスモデルにおける癌幹細胞の発見

次に、ATL 細胞浸潤を抑制するだけでなく、その増殖を抑制することができる薬剤を探索するために ATL 細胞で恒常的に活性化している NF-κB 経路を特異的に阻害する薬剤治療効果の検討を行った。しかしながら、この薬剤は *In vitro* においては mATL 細胞の NF-κB 活性化を抑制しアポトーシスを誘導する事ができるにも関わらず、*In vivo* の実験では投薬中は mATL 細胞の増殖を抑制するものの投薬の中止と共に腫瘍細胞の増殖が見られる事が明らかになった。近年、さまざまな固形腫瘍、血液腫瘍において「腫瘍内において自己複製能と腫瘍を構成するさまざ

まな分化系統の癌細胞を生み出す能力をあわせもつ細胞」と定義され高い薬剤耐性能力を有する癌幹細胞(Cancer Stem Cell; CSC)の存在が報告されている。ATL マウスモデルでは、*In vivo* において薬剤効果が著しく減じるという結果から、mATL 細胞の中には、薬剤に耐性のある Minor population が存在し、その集団が生体内での腫瘍の拡大に寄与しているのではないかという仮説が考えられた。そこで mATL 細胞を段階希釈して免疫不全マウスに移植する実験を行ったところ、10000 個の細胞移植した個体では腫瘍が再構築されるが、1000 個の細胞移植した個体では腫瘍再構築率が著しく減少した。このことから mATL 細胞中には、0.01%〜0.1%の比率で高い腫瘍再構築能を持った癌幹細胞(CSC)が存在していることが考えられた。さらに mATL 細胞の表面抗原を詳細に検討することによって、mATL 細胞中には side population に分画され、CD38(-), CD71(-), CD117(+)という表面抗原を有し、100 個の細胞移植により腫瘍を再構築する事が出来きる癌幹細胞が約 0.03%存在することが明らかになった[8]。ヒト ATL においては、マウスモデルで見つかったような癌幹細胞は未だ見つかっていない。しかしながら、他の血液腫瘍で癌幹細胞が発見されていることや ATL の治療抵抗性を考慮すると ATL に癌幹細胞が存在する事は十分考えられる事であり、現在、渡邉らが中心となって全国共同研究組織 JSPFAD によって構築されたマテリアルバンクを用いたヒト ATL での癌幹細胞の探索が行われている。

癌幹細胞の発見が大きなインパクトを持つのは、それが癌治療を根本的に変える可能性があるからである。一般的に癌幹細胞を標的とした治療法は、癌幹細胞の自己複製に必要な分子を阻害する、癌幹細胞特異的に発現する細胞表面抗原に対する抗体医薬により癌幹細胞を免疫学的に除去する、化学療法に抵抗性であった癌幹細胞の感受性を上げる、などの戦略での開発が行われている。これらの方法の鍵となるのは正常の細胞、幹細胞に極力影響を与えないような治療標的となる癌幹細胞特異的な分子を同定することである。そこで、我々は、mATL 細胞の中から CD38(-), CD71(-), CD117(+)という特徴を持つ細胞集団を集め癌幹細胞に特異的な分子の同定を質量分析計定量解析により試みている。これまでのところ癌幹細胞では非癌幹細胞に比べ、いくつかの膜タンパク質の発現が高いことが分かっている。今後、これらの分子と癌幹細胞の関係性を詳細に明らかにしていくことにより、癌幹細胞に対する特異的治療法開発につながると考えられる。

ATL に癌幹細胞が存在するという仮説の妥当性についてはヒト材料を用いた研究の結果を待つ必要があるが、このような方向の研究の潮流を創出した ATL マウスモデル研究の意義は大きい。最近、ATL マウスモデルで有効性が確認された亜ヒ酸と IFNα の併用療法は癌幹細胞に分化を誘導することによって効果があると考えられており[9]、今後、癌幹細胞に焦点を当てた研究が進むことにより ATL に対する新規治療法の開発が期待される。

おわりに

30 年以上前に ATL の発見から始まった HTLV-1 研究は、その後、ATL を含む HTLV-1 関連疾患の理解に向けてウイルス学、病理学、血液学、神経学、分子生物学など多くの分野で様々な成果が報告されてきた。しかしながら、感染から発症までの長いタイムラグと発症率の低さから HTLV-1 関連疾患を HTLV-1 感染症として捉える視点が不十分だったのではないかということが言

われている[10]。現在、その反省を踏まえ、ATL を含めた HTLV-1 関連疾患の原点は感染症であることを再認識し、感染防止ワクチンの開発やキャリア期における積極的な薬物療法の開発が試みられている。さらに、キャリアにおいて ATL 発症危険因子である末梢血リンパ球中の感染細胞比率が４％以上に増加した状態で何らかの基礎疾患に罹患している状態を示す新たな疾患概念として「慢性 HTLV-1 感染症」を定義し、この時期に HTLV-1 関連疾患発症を防止する戦略を構築することが提案されている[10]。今後、ATL を含め HTLV-1 感染症への包括的な対策を推進するためにも HTLV-1 と疾患をつなぐ「病理」を明らかにしていく必要があり、病理臨床と病理学研究の双方の立場からさらなる知見の蓄積が望まれる。

文献

1. Poiesz, B.J., F.W. Ruscetti, A.F. Gazdar, et al.: Detection and isolation of type C retrovirus particles from fresh and cultured lymphocytes of a patient with cutaneous T-cell lymphoma. Proc Natl Acad Sci U S A, 1980,77: 7415-9

2. Uchiyama, T., J. Yodoi, K. Sagawa, et al.: Adult T-cell leukemia: clinical and hematologic features of 16 cases. Blood, 1977,50: 481-92

3. 山口一成: 本邦における HTLV-1 感染および関連疾患の実態調査と総合対策. 厚生労働科学研究費補助金平成 21 年度研究統括報告書, 2010,1-25

4. 大島孝一, 新野大介: 成熟 T 細胞リンパ腫・ATLL. 病理と臨床, 2010,28: 813-820

5. Lairmore, M.D., L. Silverman, and L. Ratner: Animal models for human T-lymphotropic virus type 1 (HTLV-1) infection and transformation. Oncogene, 2005,24: 6005-15

6. Hasegawa, H., H. Sawa, M.J. Lewis, et al.: Thymus-derived leukemia-lymphoma in mice transgenic for the Tax gene of human T-lymphotropic virus type I. Nat Med, 2006,12: 466-72

7. Kawaguchi, A., Y. Orba, T. Kimura, et al.: Inhibition of the SDF-1alpha-CXCR4 axis by the CXCR4 antagonist AMD3100 suppresses the migration of cultured cells from ATL patients and murine lymphoblastoid cells from HTLV-I Tax transgenic mice. Blood, 2009,114: 2961-8

8. Yamazaki, J., T. Mizukami, K. Takizawa, et al.: Identification of cancer stem cells in a Tax-transgenic (Tax-Tg) mouse model of adult T-cell leukemia/lymphoma. Blood, 2009,114: 2709-20

9. El Hajj, H., M. El-Sabban, H. Hasegawa, et al.: Therapy-induced selective loss of leukemia-initiating activity in murine adult T cell leukemia. J Exp Med, 2010,207: 2785-92

10. 山口一成: HTLV-1 感染症ー現状と対策ー. 血液事業, 2012,35: 230-231

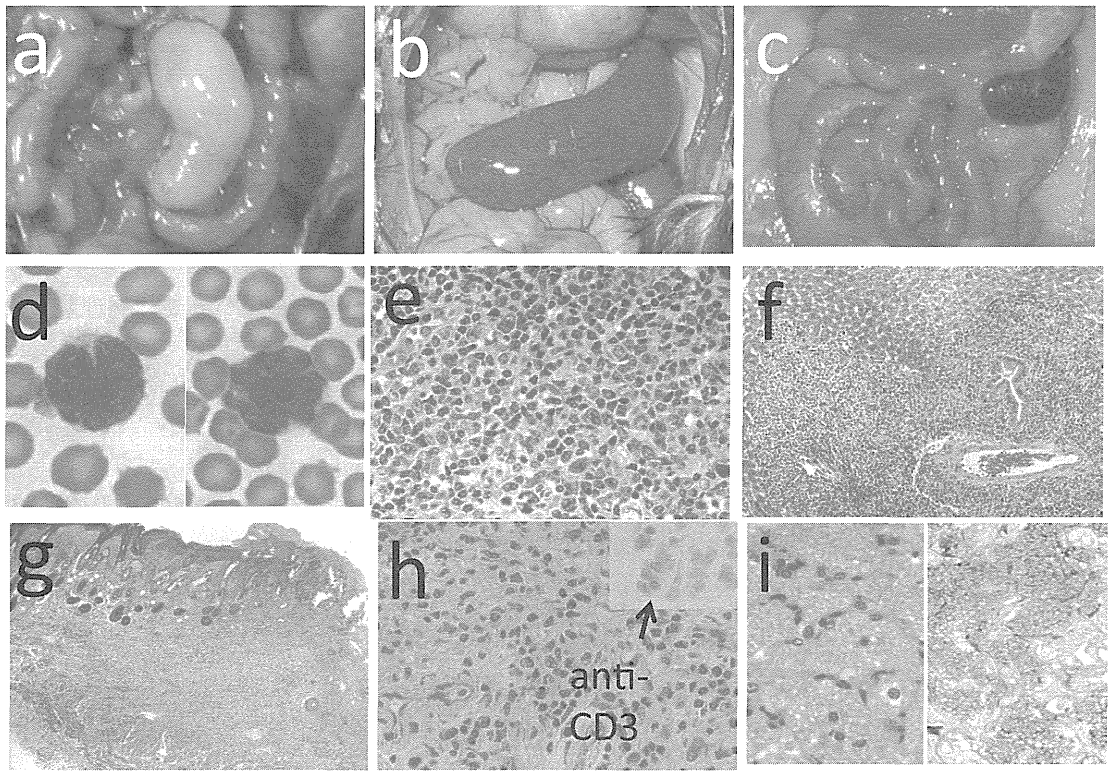

Tax Tgマウスは生後約10~23ヶ月を経過した後、リンパ腫・白血病を発症する。発症したマウスの病理所見。a) 腸間膜リンパ節の著明な腫大がみられる。b) 脾臓はコントロール(c)と比して著明な腫大がみられる。 d)末梢血ではフラワー細胞様の異型細胞を認める。e) 腸間膜リンパ節組織像。多型性の強い異型細胞を認める。f) 肝臓、g)皮膚等全身臓器への浸潤がみられる。h) 腫瘍細胞は免疫染色でCD3陽性である(図は皮膚浸潤部)。i) 発症個体ではときにニューモシスチス肺炎の合併がみられる(右:グロコット染色)

Vaccine 29 (2011) 8557–8563

Contents lists available at SciVerse ScienceDirect

Vaccine

journal homepage: www.elsevier.com/locate/vaccine

Intranasal Sendai viral vector vaccination is more immunogenic than intramuscular under pre-existing anti-vector antibodies

Chikaya Moriya[a,b], Satoshi Horiba[a], Kyoko Kurihara[a,c], Takeo Kamada[a], Yusuke Takahara[a,c], Makoto Inoue[d], Akihiro Iida[d], Hiroto Hara[d], Tsugumine Shu[d], Mamoru Hasegawa[d], Tetsuro Matano[a,c,*]

[a] The Institute of Medical Science, The University of Tokyo, 4-6-1 Shirokanedai, Minato-Ku, Tokyo 108-8639, Japan
[b] Research Team for Advanced Biologicals, National Agriculture and Food Research Organization, National Institute of Animal Health, Kannondai 3-1-5, Tsukuba 305-0856, Japan
[c] AIDS Research Center, National Institute of Infectious Diseases, 1-23-1 Toyama, Shinjuku-ku, Tokyo 162-8640, Japan
[d] DNAVEC Corporation, 6 Okubo, Tsukuba 300-2611, Japan

ARTICLE INFO

Article history:
Received 5 July 2011
Received in revised form 5 September 2011
Accepted 8 September 2011
Available online 20 September 2011

Keywords:
CD8+ T-cell responses
Sendai virus vector
Intranasal
Pre-existing antibody
AIDS vaccine

ABSTRACT

Viral vectors are promising vaccine tools for eliciting potent cellular immune responses. Pre-existing anti-vector antibodies, however, can be an obstacle to their clinical use in humans. We previously developed a Sendai virus (SeV) vector vaccine and showed the potential of this vector for efficient CD8+ T-cell induction in macaques. Here, we investigated the immunogenicity of SeV vector vaccination in the presence of anti-SeV antibodies. We compared antigen-specific CD8+ T-cell responses after intranasal or intramuscular immunization with a lower dose (one-tenth of that in our previous studies) of SeV vector expressing simian immunodeficiency virus Gag antigen (SeV-Gag) between naive and pre-SeV-infected cynomolgus macaques. Intranasal SeV-Gag immunization efficiently elicited Gag-specific CD8+ T-cell responses not only in naive but also in pre-SeV-infected animals. In contrast, intramuscular SeV-Gag immunization induced Gag-specific CD8+ T-cell responses efficiently in naive but not in pre-SeV-infected animals. These results indicate that both intranasal and intramuscular SeV administrations are equivalently immunogenic in the absence of anti-SeV antibodies, whereas intranasal SeV vaccination is more immunogenic than intramuscular in the presence of anti-SeV antibodies. It is inferred from a recent report investigating the prevalence of anti-SeV antibodies in humans that SeV-specific neutralizing titers in more than 70% of people are no more than those at the SeV-Gag vaccination in pre-SeV-infected macaques in the present study. Taken together, this study implies the potential of intranasal SeV vector vaccination to induce CD8+ T-cell responses even in humans, suggesting a rationale for proceeding to a vaccine clinical trial using this vector.

1. Introduction

Virus-specific CD8+ T-cell responses are crucial for the control of human immunodeficiency virus (HIV) and simian immunodeficiency virus (SIV) replication [1–6]. Efficient induction of virus-specific CD8+ T-cell responses is an important strategy for AIDS vaccine development, and recombinant viral vectors are promising vaccine tools for CD8+ T-cell induction [7,8]. Recent studies have indicated the potential of prophylactic viral vector immunization to induce virus-specific CD8+ T-cell responses and reduce postchallenge viral loads in macaque AIDS models [9–13]. Most of the parental or related viruses of these vectors can induce natural infection in humans. Thus, pre-existing antibodies against the vector virus itself could be an obstacle to viral vector-based CD8+ T-cell induction in humans. Indeed, a clinical trial of a vaccine using adenovirus serotype 5 (AdV5) vectors has shown reduction in efficiency of vaccine-based CD8+ T-cell induction in people with pre-existing anti-AdV5 antibodies [14–17].

We previously developed an AIDS vaccine using a recombinant Sendai virus (SeV) vector and showed that intranasal SeV vector immunization results in efficient induction of antigen-specific CD8+ T-cell responses in macaques [9,18,19]. SeV, murine parainfluenza virus type 1 (PIV-1), is an enveloped virus with a negative-sense RNA genome. SeV replication is localized in the airway because it requires a protease localized in the airway epithelium for envelope protein processing [20]. Thus, replication-competent SeV vectors [21] have been administered intranasally, while replication-defective SeV vectors [22] may be administered intramuscularly as well as intranasally. However, we have not

* Corresponding author at: AIDS Research Center, National Institute of Infectious Diseases, 1-23-1 Toyama, Shinjuku-ku, Tokyo 162-8640, Japan.
Tel.: +81 3 5285 1111; fax: +81 3 5285 1165.
E-mail addresses: tmatano@nih.go.jp, matano@ims.u-tokyo.ac.jp (T. Matano).

0264-410X/$ – see front matter © 2011 Elsevier Ltd. All rights reserved.
doi:10.1016/j.vaccine.2011.09.028

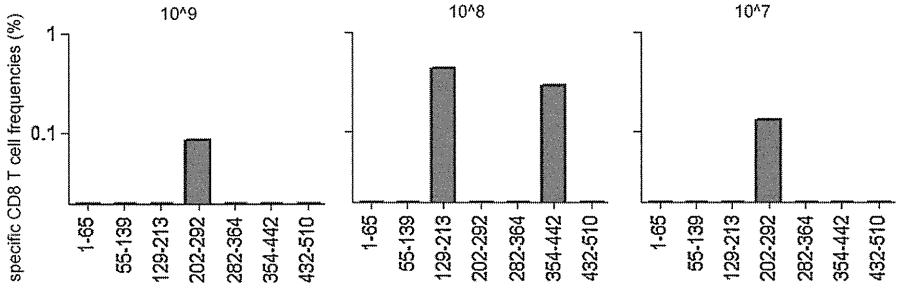

Fig. 1. Gag-specific CD8$^+$ T-cell responses after intranasal boost with lower doses of F(−)SeV-Gag. Cynomolgus macaques received a DNA vaccination, and six weeks later, were intranasally boosted with 6×10^9 ($10\hat{9}$), 6×10^8 ($10\hat{8}$), or 6×10^7 ($10\hat{7}$) CIU of F(−)SeV-Gag, respectively. Gag peptide pool-specific CD8$^+$ T-cell frequencies (percent in CD8$^+$ T lymphocytes) two weeks after the boost are shown. A panel of overlapping peptides spanning the entire SIV Gag amino acid (aa) sequence was divided into 7 pools, 1–65 (corresponding to the 1st–65th aa in SIV Gag), 55–139 (55th–139th aa), 129–213 (129th–213th aa), 202–292 (202nd–292nd aa), 282–364 (282nd–364th aa), 354–442 (354th–442nd aa), and 432–510 (432nd–510th aa), and used for the stimulation to detect peptide pool-specific CD8$^+$ T cells, respectively.

yet examined the immunogenicity of intramuscular SeV vector vaccination.

The natural host of SeV is mice and its natural infection has not been observed in primates including humans [20]. Antibodies against human PIV-1 (hPIV-1), whose natural infection frequently occurs in humans, are known to cross-react with SeV [23,24]. Our recent analyses in macaques showed efficient Gag-specific CD8$^+$ T-cell induction by an intranasal immunization with 6×10^9 CIU of F(−)SeV-Gag more than one year after an initial SeV vector inoculation, suggesting a possibility of antigen-specific CD8$^+$ T-cell induction by SeV vector administration in the presence of SeV-specific neutralizing antibody (NAb) responses [25,26]. However, it remains unclear to what extent SeV-specific NAbs could have adverse effect on CD8$^+$ T-cell induction by SeV vector vaccination.

In the present study, we investigated antigen-specific CD8$^+$ T-cell responses after intranasal or intramuscular immunization with a lower dose of SeV vector in macaques pre-infected with SeV to sensitively examine the effect of pre-SeV-infection on SeV-based CD8$^+$ T-cell induction. Our results revealed that intranasal SeV administration is more immunogenic than intramuscular in the presence of anti-SeV NAbs and suggested the potential of this vector to induce antigen-specific CD8$^+$ T-cell responses even in humans.

2. Materials and methods

2.1. Animal experiments

The animal experiments were conducted through the Cooperative Research Program in Tsukuba Primate Research Center (TPRC), National Institute of Biomedical Innovation with the help of the Corporation for Production and Research of Laboratory Primates. All animals were maintained in accordance with the guidelines for laboratory animals of the National Institute of Infectious Diseases. Blood collection and vaccination were performed under ketamine anesthesia. Cynomolgus macaques (*Macaca fascicularis*) of the TPRC breeding colonies derived from Indonesia, Malaysia, and the Philippines were used for this experiment. All animals received a DNA vaccine followed by a single boost with a replication-defective (non-transmissible) F-deleted SeV expressing SIVmac239 Gag, F(−)SeV-Gag, as described previously [9]. The DNA, CMV-SHIVdEN, used for the vaccination was constructed from an *env*- and *nef*-deleted $SHIV_{MD14YE}$ molecular clone DNA [27] and has the genes encoding SIVmac239 Gag, Pol, Vif, and Vpx, SIVmac239-HIV-1 chimeric Vpr, and HIV-1 Tat and Rev [19]. At the DNA vaccination, animals received 5 mg of CMV-SHIVdEN DNA intramuscularly. Six weeks after the DNA prime, animals intranasally or intramuscularly received a single boost with 6×10^7, 6×10^8, or 6×10^9 cell infectious units (CIU) of F(−)SeV-Gag [22,28]. Group II and IV animals were intranasally infected with 1×10^8 CIU of replication-competent (transmissible) V-knocked-out SeV [18,21] nine weeks before the DNA prime.

2.2. Measurement of Gag-specific CD8$^+$ T-cell responses

We measured Gag-specific CD8$^+$ T-cell levels by flow-cytometric analysis of gamma interferon (IFN-γ) induction after specific stimulation as described previously [9]. Peripheral blood mononuclear cells (PBMCs) were cocultured with autologous herpesvirus papio-immortalized B lymphoblastoid cell lines (B-LCLs) pulsed with peptide pools using panels of 117 overlapping peptides (mostly 15-mer) spanning the entire SIVmac239 Gag amino acid sequences [25] (Fig. 1) or a vaccinia virus vector expressing SIVmac239 Gag (Figs. 3 and 4) for Gag peptide pool-specific or Gag-specific stimulation. Intracellular IFN-γ staining was performed using CytofixCytoperm kit (BD, Tokyo, Japan) and the following monoclonal antibodies: fluorescein isothiocyanate (FITC)-conjugated anti-human CD4 (BD, #556615, M-T477), peridinin chlorophyll protein (PerCP)-conjugated anti-human CD8 (BD, #347314, SK1), allophycocyanin (APC)-conjugated anti-human CD3 (BD, #557597, SP34-2), and phycoerythrin (PE)-conjugated anti-human IFN-γ antibodies (BD, #557074, 4S.B3). Specific CD8$^+$ T-cell levels were calculated by subtracting non-specific IFN-γ$^+$ CD8$^+$ T-cell frequencies from those after Gag peptide pool-specific or Gag-specific stimulation. Specific CD8$^+$ T-cell levels less than 0.02% of CD8$^+$ T lymphocytes were considered negative.

2.3. Measurement of anti-SeV IgG levels

The plasma anti-SeV immunoglobulin G (IgG) levels were measured by an enzyme-linked immunosorbent assay (ELISA) (Denka Seiken, Tokyo, Japan) using whole inactivated SeV (HVJ Z strain) particles and a peroxidase-conjugated anti-monkey IgG antibody [29].

2.4. Measurement of anti-SeV neutralizing titers

We measured plasma SeV-specific neutralizing titers on LLC-MK2 cells using a recombinant SeV expressing enhanced green

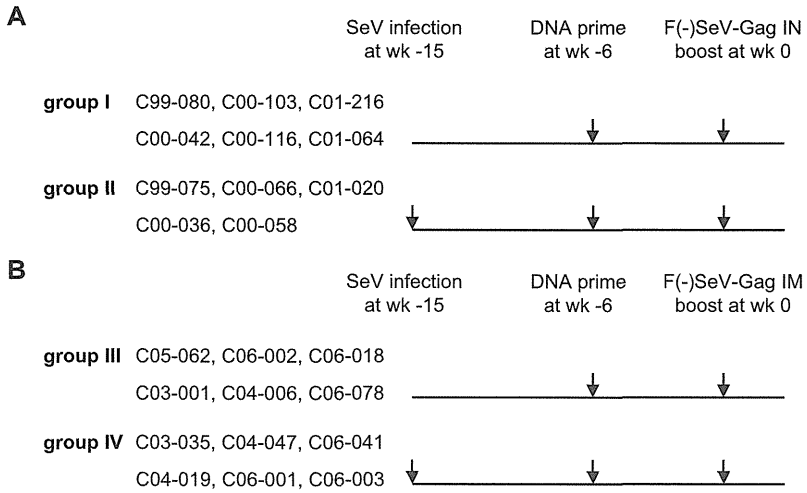

Fig. 2. Experimental protocols. (A) Groups I and II with intranasal F(−)SeV-Gag boost. Groups I ($n=6$) and II ($n=5$) received a DNA prime followed by an intranasal F(−)SeV-Gag boost. Group II animals were infected intranasally with SeV fifteen weeks before the boost. (B) Groups III and IV with intramuscular F(−)SeV-Gag boost. Groups III ($n=6$) and IV ($n=6$) received a DNA prime followed by an intramuscular F(−)SeV-Gag boost. Group IV animals were infected intranasally with SeV fifteen weeks before the boost.

fluorescent protein (SeV-EGFP) [30] as described before [26]. We determined the end-point plasma titers required for 10-fold reduction of SeV-EGFP infectivity compared to the negative control without plasma (90% neutralization titer; 90% effective concentration [EC_{90}]).

2.5. Statistical analysis

Statistical analysis was performed by Prism software version 4.03 with significance levels set at $p<0.05$ (GraphPad Software, Inc., San Diego, CA). $CD8^+$ T-cell and antibody levels were

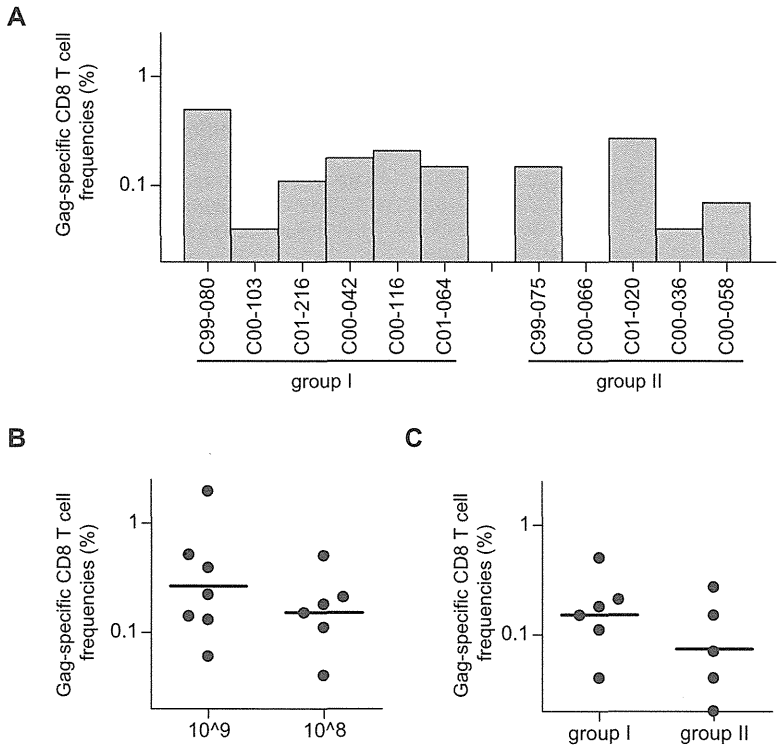

Fig. 3. Gag-specific $CD8^+$ T-cell frequencies after intranasal F(−)SeV-Gag boost in naive and pre-SeV-infected cynomolgus macaques. Gag-specific $CD8^+$ T-cell responses were examined by detection of IFN-γ induction after stimulation by B-LCLs infected with a vaccinia virus vector expressing SIVmac239 Gag. (A) Gag-specific $CD8^+$ T-cell frequencies (percent in $CD8^+$ T lymphocytes) two weeks after the boost in groups I and II. (B) Comparison of Gag-specific $CD8^+$ T-cell frequencies after boost in previously reported animals boosted with 6×10^9 of F(−)SeV-Gag ($10\hat{9}$) [31] and group II animals boosted with 6×10^8 of F(−)SeV-Gag ($10\hat{8}$) (geometric means: 0.266% in $10\hat{9}$ and 0.152% in $10\hat{8}$). (C) Comparison of Gag-specific $CD8^+$ T-cell frequencies after boost in naive (group I) and pre-SeV-infected (group II) animals (geometric means: 0.152% in group I and 0.074% in group II).

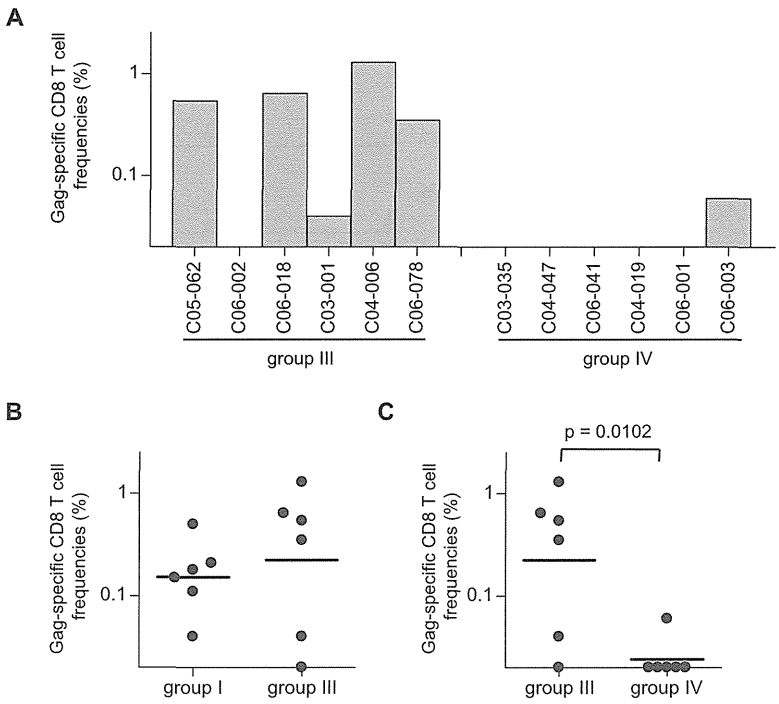

Fig. 4. Gag-specific CD8$^+$ T-cell frequencies after intramuscular F(−)SeV-Gag boost in naive and pre-SeV-infected cynomolgus macaques. (A) Gag-specific CD8$^+$ T-cell frequencies (percent in CD8$^+$ T lymphocytes) two weeks after the boost in groups III and IV. (B) Comparison of Gag-specific CD8$^+$ T-cell frequencies after boost in groups I and III. (C) Comparison of Gag-specific CD8$^+$ T-cell frequencies after boost in groups III and IV (geometric means: 0.224% in group III and 0.024% in group IV; $p = 0.0102$ by unpaired t-test [$p = 0.0260$ by Mann–Whitney's test]).

log-transformed and compared by unpaired two-tailed t test and Mann–Whitney's test.

3. Results

3.1. Gag-specific CD8$^+$ T-cell responses after intranasal F(−)SeV-Gag immunization

Our vaccine protocol consists of a single intramuscular DNA prime followed by a single boost with a replication-defective F-deleted SeV vector expressing SIVmac239 Gag, F(−)SeV-Gag, 6 weeks after the prime. In our previous studies, macaques were intranasally boosted with 6×10^9 CIU of F(−)SeV-Gag [28,31]. In the present study, we attempted vaccination with lower doses, 6×10^8 CIU (1/10 of usual dose), of F(−)SeV-Gag to sensitively examine the effect of anti-SeV antibodies on SeV-based CD8$^+$ T-cell induction. In a preliminary experiment, we confirmed Gag-specific CD8$^+$ T-cell induction by not only 6×10^8 CIU but also 6×10^7 CIU (1/100 of usual dose) of F(−)SeV-Gag boost in cynomolgus macaques (Fig. 1). Then, we examined the immunogenicity of 6×10^8 CIU of F(−)SeV-Gag in the present study.

Twenty-three cynomolgus macaques were divided into four groups. Groups I ($n = 6$) and II ($n = 5$) received a F(−)SeV-Gag boost intranasally whereas groups III ($n = 6$) and IV ($n = 6$) received it intramuscularly (Fig. 2). Groups II and IV were intranasally pre-infected with SeV fifteen weeks before the boost. No animals showed detectable Gag-specific CD8$^+$ T-cell responses at week 0, just before the boost.

In group I, all six animals efficiently elicited Gag-specific CD8$^+$ T-cell responses after the intranasal boost (Fig. 3A). There was no significant difference in Gag-specific CD8$^+$ T-cell levels between the group I boosted with 6×10^8 CIU of F(−)SeV-Gag and the animals ($n = 7$) boosted with 6×10^9 CIU of F(−)SeV-Gag in our previous study [31] (Fig. 3B), confirming the immunogenicity of F(−)SeV-Gag boost at the dose of 6×10^8 CIU. In group II, efficient Gag-specific CD8$^+$ T-cell responses were observed in four animals except for one (Fig. 3A). No significant difference in Gag-specific CD8$^+$ T-cell levels was observed between groups I and II (Fig. 3C). These results indicate that the intranasal boost with the lower dose (6×10^8 CIU) of F(−)SeV-Gag can elicit Gag-specific CD8$^+$ T-cell responses even in pre-SeV-infected macaques.

3.2. Gag-specific CD8$^+$ T-cell responses after intramuscular F(−)SeV-Gag immunization

Five animals except for one in group III showed efficient Gag-specific CD8$^+$ T-cell response after the intramuscular F(−)SeV-Gag boost (Fig. 4A). The Gag-specific CD8$^+$ T-cell levels in group III were similar to those in group I (Fig. 4B), confirming the immunogenicity of intramuscular F(−)SeV-Gag boost. In contrast, group IV macaques failed to induce Gag-specific CD8$^+$ T-cell responses efficiently; only one of six animals induced detectable responses (Fig. 4A). The Gag-specific CD8$^+$ T-cell levels in group IV were significantly reduced compared to those in group III (Fig. 4C) and those in group II ($p = 0.0302$). These results indicate that the intramuscular F(−)SeV-Gag boost can elicit Gag-specific CD8$^+$ T-cell responses efficiently in SeV-uninfected but not in pre-SeV-infected macaques.

3.3. SeV-specific antibody responses after F(−)SeV-Gag immunization

We then examined SeV-specific antibody responses. All pre-SeV-infected animals in groups II and IV had similar levels of SeV-binding antibodies in plasma at week 0, just before the F(−)SeV-Gag boost (Figs. 5 and 6). SeV-specific neutralization assay showed similar levels of SeV-specific NAb responses at week 0 in

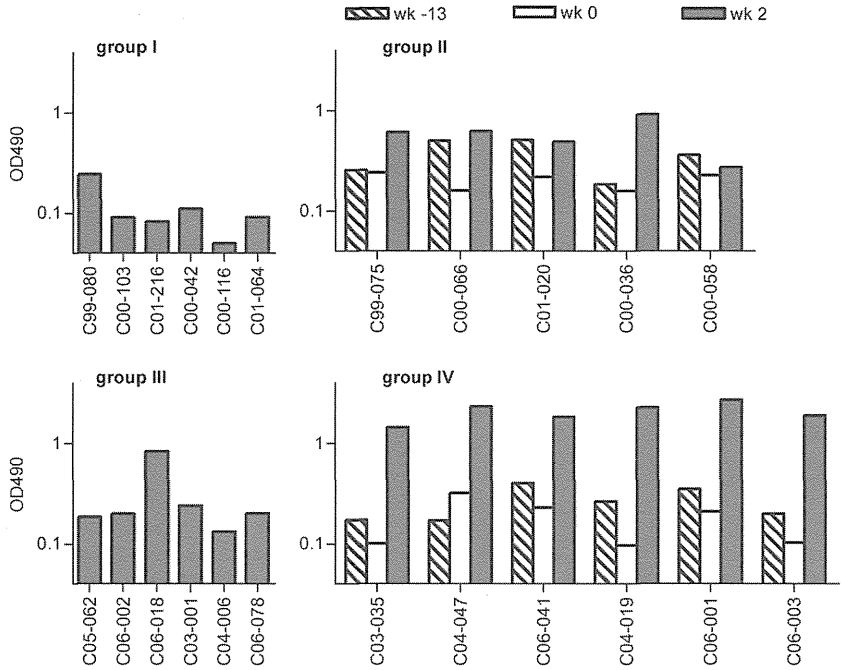

Fig. 5. SeV-specific IgG levels in plasma. Plasma samples obtained from group I and III animals at week 2 and those from group II and IV animals at weeks −13, 0 and 2 were diluted by 1/5000 and subjected to ELISA assay. OD490, optical density at 490 nm.

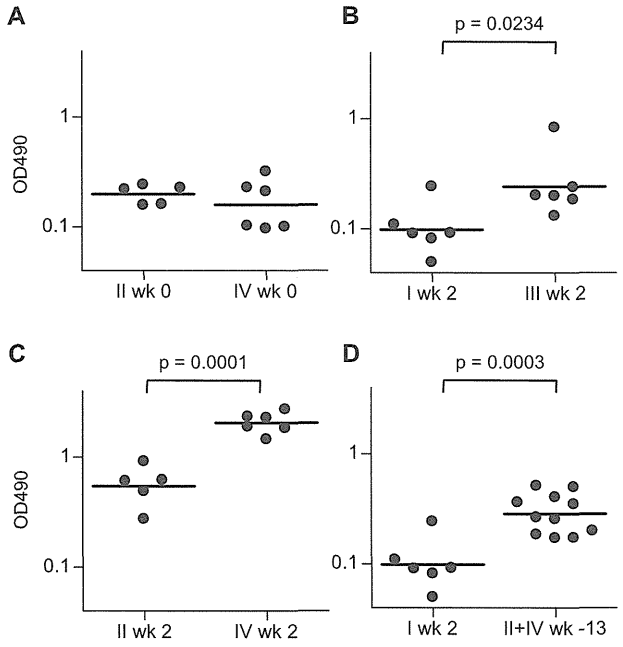

Fig. 6. Comparison of plasma SeV-specific IgG levels among groups. (A) Comparison of plasma SeV-specific IgG levels at week 0, just before F(−)SeV-Gag boost, in groups II and IV (geometric means: 0.199 in group II and 0.159 in group IV). (B) Comparison of plasma SeV-specific IgG levels at week 2, two weeks after the boost, in groups I and III (geometric means: 0.099 in group I and 0.242 in group III; $p = 0.0234$ by unpaired t-test [$p = 0.0411$ by Mann–Whitney's test]). (C) Comparison of plasma SeV-specific IgG levels at week 2 in groups II and IV (geometric means: 0.542 in group II and 2.051 in group IV; $p = 0.0001$ by unpaired t-test [$p = 0.0043$ by Mann–Whitney's test]). (D) Comparison of plasma SeV-specific IgG levels at week 2 in group I and at week −13, two weeks after SeV infection, in groups II and IV (geometric means: 0.285 in groups II and IV; $p = 0.0003$ by unpaired t-test [$p = 0.0042$ by Mann–Whitney's test]).

groups II and IV (Fig. 7); the 90% neutralizing titers were 25–100 and their geometric means were 57 and 56, respectively. Thus, even in the presence of these levels of anti-SeV NAbs, intranasal but not intramuscular administration with 6×10^8 CIU of F(−)SeV-Gag can efficiently elicit Gag-specific $CD8^+$ T-cell responses in macaques.

Plasma SeV-specific IgG levels at week 2, two weeks after F(−)SeV-Gag boost, in group I were significantly lower than those in group III (Fig. 6B). The F(−)SeV-Gag boost enhanced SeV-specific antibody responses in all the pre-SeV-infected animals. Plasma SeV-specific IgG levels two weeks after the boost in group II were significantly lower than in group IV (Fig. 6C). Neutralization assay confirmed these results; SeV-specific NAb titers two weeks after F(−)SeV-Gag boost in group I were significantly lower than in group III (Fig. 7B) and those in group II were significantly lower than in group IV (Fig. 7C). These results indicate that intranasal F(−)SeV-Gag vaccination induces plasma SeV-specific antibody responses less efficiently than intramuscular F(−)SeV-Gag vaccination. Finally, SeV-specific IgG levels and NAb titers at week −13, two weeks after SeV infection, in groups II and IV were higher than those at week 2, two weeks after intranasal F(−)SeV-Gag boost, in group I (Figs. 6D and 7D), suggesting less efficient induction of plasma SeV-specific antibody responses by intranasal replication-defective F(−)SeV-Gag immunization than replication-competent SeV.

4. Discussion

In the present study, we first confirmed that an intranasal boost even with a lower dose (6×10^8 CIU, one-tenth of that in our usual protocol) of F(−)SeV-Gag can induce Gag-specific $CD8^+$ T-cell responses efficiently in macaques. We then showed immunogenicity of the intranasal boost with this lower dose of F(−)SeV-Gag in the presence of SeV-specific NAbs in pre-SeV-infected macaques; Gag-specific $CD8^+$ T-cell responses were induced by the boost fifteen weeks after SeV infection.

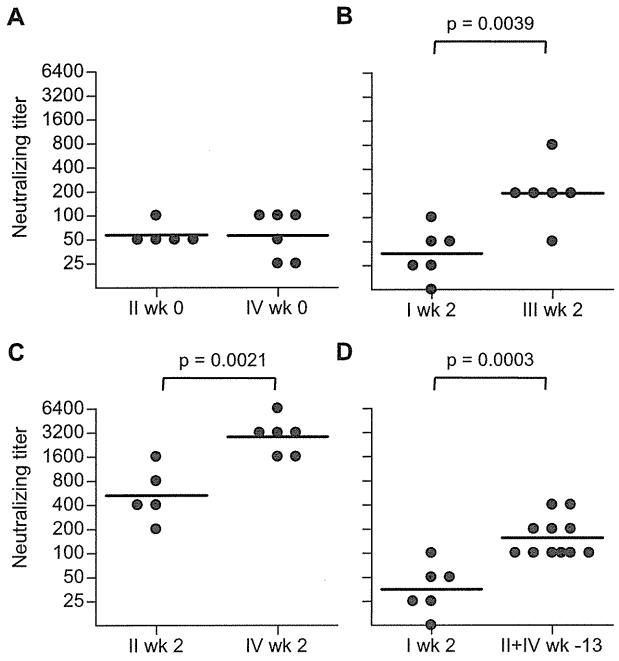

Fig. 7. Comparison of plasma SeV-specific NAb titers among groups. (A) Comparison of plasma SeV-specific NAb titers at week 0 in groups II and IV (geometric means: 5.7×10^1 in group II and 5.6×10^1 in group IV). (B) Comparison of plasma SeV-specific NAb titers at week 2 in groups I and III (geometric means: 3.5×10^1 in group I and 2.0×10^2 in group III; $p = 0.0039$ by unpaired t-test [$p = 0.0087$ by Mann–Whitney's test]). (C) Comparison of plasma SeV-specific NAb titers at week 2 in groups II and IV (geometric means: 5.3×10^2 in group II and 2.9×10^3 in group IV; $p = 0.0021$ by unpaired t-test [$p = 0.0087$ by Mann–Whitney's test]). (D) Comparison of plasma SeV-specific NAb titers at week 2 in group I and at week −13 in groups II and IV (geometric means: 1.6×10^2 in groups II and IV; $p = 0.0003$ by unpaired t-test [$p = 0.0029$ by Mann–Whitney's test]).

SeV has homology in viral genome sequences with hPIV-1, averaging 75% across the six viral genes [32]. Naturally acquired human antibody responses to hPIV-1 cross-react with SeV. A recent study investigating the prevalence of anti-SeV NAbs in humans in Africa, Europe, United States, and Japan [33] detected anti-SeV NAbs in 92.5% subjects with a median titer of 60.6; the 50% neutralization titers (EC_{50}) were measured on LLC-MK2 cells by determining the end-point plasma titers required for 2-fold reduction of SeV-GFP infection. The majority had titers less than 1000 with 71.7% less than 100. Therefore, it is inferred that, in more than 70% of people, anti-SeV NAb titers are no more than those observed just before the F(−)SeV-Gag boost in groups II in the present study. Although it remains unclear whether an intranasal immunization with the lower dose (6×10^8 CIU) or the usual dose (6×10^9 CIU) of SeV vector can work in those with 50% anti-SeV NAb titers of 100–1000, these results imply the potential of SeV vector to induce $CD8^+$ T-cell responses even in humans.

SeV vector has been used for gene transfer and efficient gene expression by its intramuscular inoculation has been shown in multiple studies [34–36]. While the immunogenicity of intramuscular SeV vector inoculation has not been determined, the present study, for the first time, has confirmed the potential of an intramuscular F(−)SeV-Gag boost to induce Gag-specific $CD8^+$ T-cell responses efficiently in SeV naive macaques. Interestingly, however, the intramuscular boost failed to elicit Gag-specific $CD8^+$ T-cell responses efficiently in pre-SeV-infected animals, indicating that both intranasal and intramuscular SeV administrations can induce antigen-specific $CD8^+$ T-cell responses equivalently in the absence of anti-SeV antibodies, whereas intranasal SeV vaccination is more immunogenic than intramuscular in the presence of plasma anti-SeV antibodies. These results possibly imply higher sensitivity of intramuscular SeV inoculation to plasma SeV-specific NAb responses, which may reflect the difference in the route and the mechanism for antigen presentation by intranasal and intramuscular SeV vector immunization in vivo. SeV-specific IgA was detectable in nasal swabs at week 0 in four of five group II macaques (except for macaque C00-058) (data not shown), although we were unable to quantify the IgA levels. Mucosal immune responses are considered important for protecting viral infection via the upper respiratory tract [37–39], but those mucosal responses at week 0 in group II did not significantly diminish $CD8^+$ T-cell induction by intranasal F(−)SeV-Gag boost in the present study.

This study showed less efficient induction of SeV-specific antibody responses by intranasal F(−)SeV-Gag immunization than intramuscular. Indeed, plasma SeV-specific IgG or NAb levels even after intranasal replication-competent SeV infection (at week −13 in groups II and IV) were not more than those after intramuscular replication-defective F(−)SeV-Gag boost (at week 2 in group III). Our results also indicated less efficient SeV-specific antibody induction by intranasal replication-defective F(−)SeV-Gag immunization than replication-competent SeV. Thus, intranasal SeV vector immunization may not induce plasma antibody responses efficiently. However, intranasal immunization with replication-defective F-deleted SeV vectors would be advantageous for repeated vaccination toward antigen-specific $CD8^+$ T-cell induction.

In summary, our results indicate that both intranasal and intramuscular SeV administrations are equivalently immunogenic in the absence of anti-SeV NAbs, whereas intranasal SeV vector vaccination is more immunogenic than intramuscular in the presence of anti-SeV NAbs. This study implies the potential of intranasal SeV vector vaccination to induce $CD8^+$ T-cell responses even in humans.

Acknowledgements

This work was supported by grants from the Ministry of Education, Culture, Sports, Science, and Technology, grants from the Ministry of Health, Labor, and Welfare, and a grant from Takeda Science Foundation in Japan. We thank H. Akari, Y. Yasutomi, F. Ono, A. Hiyaoka, K. Komatsuzaki, K. Oto, and H. Ogawa for their assistance in animal experiments.

References

[1] Koup RA, Safrit JT, Cao Y, Andrews CA, Mcleod G, Borkowsky W, et al. Temporal association of cellular immune responses with the initial control of viremia in primary human immunodeficiency virus type 1 syndrome. J Virol 1994;68:4650–5.
[2] Borrow P, Lewicki H, Hahn BH, Shaw GM, Oldstone MB. Virus-specific $CD8^+$ cytotoxic T-lymphocyte activity associated with control of viremia in primary human immunodeficiency virus type 1 infection. J Virol 1994;68:6103–10.
[3] Matano T, Shibata R, Siemon C, Connors M, Lane HC, Martin MA. Administration of an anti-CD8 monoclonal antibody interferes with the clearance of chimeric simian/human immunodeficiency virus during primary infections of rhesus macaques. J Virol 1998;72:164–9.
[4] Jin X, Bauer DE, Tuttleton SE, Lewin S, Gettie A, Blanchard J, et al. Dramatic rise in plasma viremia after $CD8^+$ T cell depletion in simian immunodeficiency virus-infected macaques. J Exp Med 1999;189:991–8.
[5] Schmitz JE, Kuroda MJ, Santra S, Sasseville VG, Simon MA, Lifton MA, et al. Control of viremia in simian immunodeficiency virus infection by $CD8^+$ lymphocytes. Science 1999;28:857–60.
[6] Goulder PJ, Watkins DI. HIV and SIV CTL escape: implications for vaccine design. Nat Rev Immunol 2004;4:630–40.
[7] McMichael AJ, Hanke T. HIV vaccines 1983–2003. Nat Med 2003;9:874–80.
[8] Koff WC, Parks CL, Berkhout B, Ackland J, Noble S, Gust ID. Replicating viral vectors as HIV vaccines: summary report from IAVI sponsored satellite symposium. Biologicals 2008;36:277–86.
[9] Matano T, Kobayashi M, Igarashi H, Takeda A, Nakamura H, Kano M, et al. Cytotoxic T lymphocyte-based control of simian immunodeficiency virus replication in a preclinical AIDS vaccine trial. J Exp Med 2004;199:1709–18.

[10] Letvin NL, Mascola JR, Sun Y, Gorgone DA, Buzby AP, Xu L, et al. Preserved CD4+ central memory T cells and survival in vaccinated SIV-challenged monkeys. Science 2006;312:1530–3.
[11] Wilson NA, Reed J, Napoe GS, Piaskowski S, Szymanski A, Furlott J, et al. Vaccine-induced cellular immune responses reduce plasma viral concentrations after repeated low-dose challenge with pathogenic simian immunodeficiency virus SIVmac239. J Virol 2006;80:5875–85.
[12] Hansen SG, Vieville C, Whizin N, Coyne-Johnson L, Siess DC, Drummond DD, et al. Effector memory T cell responses are associated with protection of rhesus monkeys from mucosal simian immunodeficiency virus challenge. Nat Med 2009;15:293–9.
[13] Liu J, O'Brien KL, Lynch DM, Simmons NL, La Porte A, Riggs AM, et al. Immune control of an SIV challenge by a T-cell-based vaccine in rhesus monkeys. Nature 2009;457:87–91.
[14] Sumida SM, Truitt DM, Lemckert AAC, Vogels R, Custers JHHV, Addo MM, et al. Neutralizing antibodies to adenovirus serotype 5 vaccine vectors are directed primarily against the adenovirus hexon protein. J Immunol 2005;174:7179–85.
[15] Catanzaro AT, Koup RA, Roederer M, Bailer RT, Enama ME, Moodie Z, et al. Phase 1 safety and immunogenicity evaluation of a multiclade HIV-1 candidate vaccine delivered by a replication-defective recombinant adenovirus vector. J Infect Dis 2006;194:1638–49.
[16] Berkley SF, Koff WC. Scientific and policy challenges to development of an AIDS vaccine. Lancet 2007;370:94–101.
[17] Priddy FH, Brown D, Kublin J, Monahan K, Wright DP, Lalezari J, et al. Safety and immunogenicity of a replication-incompetent adenovirus type 5 HIV-1 clade B gag/pol/nef vaccine in healthy adults. Clin Infect Dis 2008;46:1769–81.
[18] Matano T, Kano M, Nakamura H, Takeda A, Nagai Y. Rapid appearance of secondary immune responses and protection from acute CD4 depletion after a highly pathogenic immunodeficiency virus challenge in macaques vaccinated with a DNA-prime/Sendai viral vector-boost regimen. J Virol 2001;75:11891–6.
[19] Kano M, Matano T, Kato A, Nakamura H, Takeda A, Suzaki Y, et al. Primary replication of a recombinant Sendai viral vector in macaques. J Gen Virol 2002;83:1377–86.
[20] Nagai Y. Paramyxovirus replication and pathogenesis. Reverse genetics transforms understanding. Rev Med Virol 1999;9:83–99.
[21] Kato A, Sakai Y, Shioda T, Kondo T, Nakanishi M, Nagai Y. Initiation of Sendai virus multiplication from transfected cDNA or RNA with negative or positive sense. Genes Cells 1996;1:569–79.
[22] Li HO, Zhu YF, Asakawa M, Kuma H, Hirata T, Ueda Y, et al. A cytoplasmic RNA vector derived from nontransmissible Sendai virus with efficient gene transfer and expression. J Virol 2000;74:6564–9.
[23] Skiadopoulos MH, Surman SR, Riggs JM, Elkins WR, St Claire M, Nishio M, et al. Sendai virus, a murine parainfluenza virus type 1, replicates to a level similar to human PIV1 in the upper and lower respiratory tract of African green monkeys and chimpanzees. Virology 2002;297:153–60.
[24] Slobod KS, Shenep JL, Lujan-Zilbermann J, Allison K, Brown B, Scroggs RA, et al. Safety and immunogenicity of intranasal murine parainfluenza virus type 1 (Sendai virus) in healthy human adults. Vaccine 2004;22:3182–6.
[25] Kato M, Igarashi H, Takeda A, Sasaki Y, Nakamura H, Kano M, et al. Induction of Gag-specific T-cell responses by therapeutic immunization with a Gag-expressing Sendai virus vector in macaques chronically infected with simian-human immunodeficiency virus. Vaccine 2005;23:3166–73.
[26] Moriya C, Horiba S, Inoue M, Iida A, Hara H, Shu T, et al. Antigen-specific T-cell induction by vaccination with a recombinant Sendai virus vector even in the presence of vector-specific neutralizing antibodies in rhesus macaques. Biochem Biophys Res Commun 2008;371:850–4.
[27] Shibata R, Maldarelli F, Siemon C, Matano T, Parta M, Miller G, et al. Infection and pathogenicity of chimeric simian-human immunodeficiency viruses in macaques: determinants of high virus loads and CD4 cell killing. J Infect Dis 1997;176:362–73.
[28] Takeda A, Igarashi H, Nakamura H, Kano M, Iida A, Hirata T, et al. Protective efficacy of an AIDS vaccine, a single DNA-prime followed by a single booster with a recombinant replication-defective Sendai virus vector, in a macaque AIDS model. J Virol 2003;77:9710–5.
[29] Yoshizaki M, Hironaka T, Iwasaki H, Ban H, Tokusumi Y, Iida A, et al. Naked Sendai virus vector lacking all of the envelope-related genes: reduced cytopathogenicity and immunogenicity. J Gene Med 2006;8: 1151–9.
[30] Kato A, Kiyotani K, Sakai Y, Yoshida T, Nagai Y. The paramyxovirus, Sendai virus, V protein encodes a luxury function required for viral pathogenesis. EMBO J 1997;16:578–87.
[31] Takeda A, Igarashi H, Kawada M, Tsukamoto T, Yamamoto H, Inoue M, et al. Evaluation of the immunogenicity of replication-competent V-knocked-out and replication-defective F-deleted Sendai virus vector-based vaccines in macaques. Vaccine 2008;26:6839–43.
[32] Takimoto T, Bousse T, Portner A. Molecular cloning and expression of human parainfluenza virus type 1 L gene. Virus Res 2000;70:45–53.
[33] Hara H, Hironaka T, Inoue M, Iida A, Shu T, Hasegawa M, et al. Prevalence of specific neutralizing antibodies against Sendai virus in populations from different geographic areas: implications for AIDS vaccine development using Sendai virus vector. Hum Vaccin 2011 [Epub ahead of print].
[34] Masaki I, Yonemitsu Y, Yamashita A, Sata S, Tanii M, Komori K, et al. Angiogenic gene therapy for experimental critical limb ischemia: acceleration of limb loss by overexpression of vascular endothelial growth factor 165 but not of fibroblast growth factor-2. Circ Res 2002;90:966–73.
[35] Huang J, Inoue M, Hasegawa M, Tomihara K, Tanaka T, Chen J, et al. Sendai viral vector mediated angiopoietin-1 gene transfer for experimental ischemic limb disease. Angiogenesis 2009;12:243–9.
[36] Kinoh H, Inoue M, Komaru A, Ueda Y, Hasegawa M, Yonemitsu Y. Generation of optimized and urokinase-targeted oncolytic Sendai virus vectors applicable for various human malignancies. Gene Ther 2009;16: 392–403.
[37] Boyce TG, Hsu HH, Sannella EC, Coleman-Dockery SD, Baylis E, Zhu Y, et al. Safety and immunogenicity of adjuvanted and unadjuvanted subunit influenza vaccines administered intranasally to healthy adults. Vaccine 2000;19: 217–26.
[38] Chen D, Periwal SB, Larrivee K, Zuleger C, Erickson CA, Endres RL, et al. Serum and mucosal immune responses to an inactivated influenza virus vaccine induced by epidermal powder immunization. J Virol 2001;75: 7956–65.
[39] Ichinohe T, Kawaguchi A, Tamura S, Takahashi H, Sawa H, Ninomiya A, et al. Intranasal immunization with H5N1 vaccine plus Poly I:Poly C12U, a Toll-like receptor agonist, protects mice against homologous and heterologous virus challenge. Microbes Infect 2007;9:1333–40.

ELSEVIER

Institut Pasteur

Microbes and Infection 14 (2012) 1169–1176

www.elsevier.com/locate/micinf

Original article

Immunogenicity of repeated Sendai viral vector vaccination in macaques

Kyoko Kurihara [a,b], Yusuke Takahara [a,b], Takushi Nomura [a,b], Hiroshi Ishii [a,b], Nami Iwamoto [a,b], Naofumi Takahashi [a,b], Makoto Inoue [c], Akihiro Iida [c], Hiroto Hara [c], Tsugumine Shu [c], Mamoru Hasegawa [c], Chikaya Moriya [b], Tetsuro Matano [a,b,*]

[a] *AIDS Research Center, National Institute of Infectious Diseases, 1-23-1 Toyama, Shinjuku-ku, Tokyo 162-8640, Japan*
[b] *The Institute of Medical Science, The University of Tokyo, 4-6-1 Shirokanedai, Minato-ku, Tokyo 108-8639, Japan*
[c] *DNAVEC Corporation, 6 Okubo, Tsukuba 300-2611, Japan*

Received 4 May 2012; accepted 21 July 2012
Available online 31 July 2012

Abstract

Induction of durable cellular immune responses by vaccination is an important strategy for the control of persistent pathogen infection. Viral vectors are promising vaccine tools for eliciting antigen-specific T-cell responses. Repeated vaccination may contribute to durable memory T-cell induction, but anti-vector antibodies could be an obstacle to its efficacy. We previously developed a Sendai virus (SeV) vector vaccine and showed the potential of this vector for efficient T-cell induction in macaques. Here, we examined whether repeated SeV vector vaccination with short intervals can enhance antigen-specific $CD8^+$ T-cell responses. Four rhesus macaques possessing the MHC-I haplotype 90-120-Ia were immunized three times with intervals of three weeks. For the vaccination, we used replication-defective F-deleted SeV vectors inducing $CD8^+$ T-cell responses specific for simian immunodeficiency virus $Gag_{206-216}$ and $Gag_{241-249}$, which are dominant epitopes restricted by 90-120-Ia-derived MHC-I molecules. All four animals showed higher $Gag_{206-216}$-specific and $Gag_{241-249}$-specific $CD8^+$ T-cell responses after the third vaccination than those after the first vaccination, indicating enhancement of antigen-specific $CD8^+$ T-cell responses by the second/third SeV vector vaccination even with short intervals. These results suggest that repeated SeV vector vaccination can contribute to induction of efficient and durable T-cell responses.

Keywords: AIDS vaccine; Viral vector; CTL; SIV

1. Introduction

Antigen-specific T-cell responses play a central role in the control of persistent infection with pathogens such as human immunodeficiency viruses (HIVs) [1–7]. Induction of efficient and durable T-cell responses is an important vaccine strategy, and recombinant viral vectors are promising vaccine tools for antigen-specific T-cell induction [8]. Many kinds of viral vectors including adenovirus (AdV) and poxvirus vectors have been shown to efficiently induce antigen-specific T-cell responses [9–14]. Repeated viral vector vaccination may induce enhanced and durable memory T-cell responses. Viral vector vaccination, however, elicits antibodies against the vector virus itself, which could be an obstacle to the potential of repeated viral vector vaccination [15].

We previously developed a vaccine system using Sendai virus (SeV) vectors to induce antigen-specific T-cell responses [16,17]. We have replication-defective (nontransmissible) F-deleted SeV, F(-)SeV, as well as replication-competent SeV vectors [18,19]. In our recent study [20], intranasal immunization even with a lower dose (6×10^8 CIU [cell infectious units]) of F(-)SeV vectors in SeV-infected macaques efficiently elicited antigen-specific $CD8^+$ T-cell responses in the presence of SeV-specific neutralizing titers of 1:50–1:100.

* Corresponding author. AIDS Research Center, National Institute of Infectious Diseases, 1-23-1 Toyama, Shinjuku-ku, Tokyo 162-8640, Japan. Tel.: +81 3 5285 1111; fax: +81 3 5285 1165.
E-mail addresses: tmatano@nih.go.jp, matano@ims.u-tokyo.ac.jp (T. Matano).

1286-4579/$ - see front matter © 2012 Institut Pasteur. Published by Elsevier Masson SAS. All rights reserved.
http://dx.doi.org/10.1016/j.micinf.2012.07.016

Intramuscular F(-)SeV vector immunization can also induce antigen-specific $CD8^+$ T-cell responses efficiently in the absence of anti-SeV neutralizing antibodies, but intranasal F(-)SeV vector vaccination is more immunogenic than intramuscular in the presence of anti-SeV neutralizing antibodies.

Thus, repeated intranasal SeV vector immunization may have the potential to overcome anti-SeV antibody responses and induce more efficient and durable T-cell responses than those by single immunization. Our previous analyses in macaques [21] showed efficient antigen-specific $CD8^+$ T-cell induction by an intranasal immunization with 6×10^9 CIU of F(-)SeV vectors more than one year after an initial SeV vector inoculation, indicating the immunogenicity of repeated SeV vector vaccination with long intervals.

In the present study, we investigated whether repeated SeV vector vaccination with short intervals can enhance antigen-specific $CD8^+$ T-cell responses. Macaques received SeV vectors intranasally and intramuscularly at the second and the third vaccination at weeks 3 and 6 after the first intranasal SeV vector vaccination. While clear difference in immunogenicity was not shown between intranasal and intramuscular SeV vector administration, all the animals exhibited higher antigen-specific $CD8^+$ T-cell responses after the third vaccination than those after the first. Our results indicate that repeated SeV vector vaccination even with short intervals can contribute to induction of efficient, durable T-cell responses.

2. Materials and methods

2.1. Animals

The animal experiments were conducted through the Cooperative Research Program in Tsukuba Primate Research Center (TPRC), National Institute of Biomedical Innovation with the help of the Corporation for Production and Research of Laboratory Primates. All animals were maintained in accordance with the guidelines for laboratory animals of the National Institute of Infectious Diseases and TPRC. Blood collection and vaccination were performed under ketamine anesthesia.

In the present study, we used four Burmese rhesus macaques possessing the major histocompatibility complex class I (MHC-I) haplotype *90-120-Ia* [22]; those *90-120-Ia*-positive macaques are known to dominantly elicit SIVmac239 $Gag_{206-216}$ (IINEEAADWDL) epitope-specific and $Gag_{241-249}$ (SSVDEQIQW) epitope-specific $CD8^+$ T-cell responses after SIVmac239 challenge [23,24]. In our previous study [25–27], these four macaques were challenged with SIV after vaccination and controlled SIV replication in the chronic phase as follows. Macaque R04-016 received a prophylactic prime-boost vaccine eliciting single $Gag_{241-249}$ epitope-specific $CD8^+$ T-cell responses before SIVmac239 challenge [26]. Macaque R04-015 received a prophylactic prime-boost vaccine eliciting $Gag_{206-216}$ epitope-specific and $Gag_{241-249}$ epitope-specific $CD8^+$ T-cell responses [27,28]. Macaques R06-015 and R06-035 received a prophylactic DNA prime/F(-)SeV-Gag boost vaccine [25].

Macaques R04-015, R04-016, and R06-015 contained a challenge with SIVmac239 [29] approximately 3 months after the boost and a superchallenge with a mutant SIVmac239 carrying five gag mutations, SIVmac239Gag216S244E247L312V373T, in the chronic phase (at week 40 [R06-015] or 116 [R04-015 and R04-016] after SIVmac239 challenge) [27]. Macaque R06-035 was challenged with a mutant SIVmac239, SIVmac239-Gag216S244E, carrying two gag mutations, GagL216S and GagD244E leading to a leucine (L)-to-serine (S) substitution at the 216th amino acid and an aspartic acid (D)-to-glutamic acid (E) substitution at the 244th in Gag [25]. These mutations result in escape from $Gag_{206-216}$-specific and $Gag_{241-249}$-specific $CD8^+$ T-cell responses. In this animal that failed to control the mutant SIV challenge, persistent viremia was observed for 8 months, but after that, plasma viremia became undetectable.

2.2. Vaccination

In the present study, macaques R04-015, R04-016, R06-015, and R06-035 received an intranasal F(-)SeV-Gag vector vaccination (referred to as the first vaccination) at weeks 128, 128, 52, and 67 after SIV challenge, respectively. At the second and the third vaccination, we used two kinds of F(-)SeV vectors, F(-)SeV-$Gag_{202-216}$-EGFP expressing $Gag_{202-216}$-EGFP fusion protein and F(-)SeV-Gag216S expressing SIVmac239 Gag with a mutation leading to escape from $Gag_{206-216}$-specific $CD8^+$ T-cell responses [23], for eliciting $Gag_{206-216}$-specific and $Gag_{241-249}$-specific $CD8^+$ T-cell responses, respectively (Fig. 1). The F(-)SeV-Gag216S is considered not to induce $Gag_{206-216}$-specific $CD8^+$ T-cell responses, because challenge of macaques with a SIV carrying this Gag216S mutation induced no $Gag_{206-216}$-specific $CD8^+$ T-cell responses in a previous study [25]. Macaques R04-015 and R06-035 received F(-)SeV-$Gag_{202-216}$-EGFP intranasally and F(-)SeV-Gag216S intramuscularly at the second vaccination three weeks after the first. At the third vaccination three weeks after the second, these animals received F(-)SeV-Gag216S intranasally and F(-)SeV-$Gag_{202-216}$-EGFP intramuscularly. On the contrary, macaques R04-016 and R06-015 received F(-)SeV-Gag216S intranasally and F(-)SeV-$Gag_{202-216}$-EGFP intramuscularly at the second vaccination and F(-)SeV-$Gag_{202-216}$-EGFP intranasally and F(-)SeV-Gag216S intramuscularly at the third. The dose of each vaccination was 6×10^9 cell infectious units (CIU). During the observation period in the present study, plasma viremia was undetectable in all four macaques.

2.3. Measurement of antigen-specific $CD8^+$ T-cell responses

We measured antigen-specific $CD8^+$ T-cell frequencies by flow-cytometric analysis of gamma interferon (IFN-γ) induction after specific stimulation as described previously [21,27]. Peripheral blood mononuclear cells (PBMCs) were cocultured with autologous herpesvirus papio-immortalized B lymphoblastoid cell lines (B-LCLs) pulsed with 1 μM $Gag_{206-216}$ or $Gag_{241-249}$ peptide for $Gag_{206-216}$-specific or $Gag_{241-249}$-specific stimulation. For SeV-specific stimulation, PBMCs were cocultured with B-LCLs infected with SeV. Intracellular IFN-γ staining was performed using CytofixCytoperm kit